Mechanistic target of rapamycin (mTOR) regulates self-sustained quiescence, tumor indolence and late clinical metastasis in a Beclin-1-dependent manner.

Carole Nicco[1], Marine Thomas[1], Julie Guillermet[2], Maryline Havard[3], Fanny Laurent-Tchenio[3], Ludivine Doridot[1], François Dautry[3], Frédéric Batteux[1], Thierry Tchenio[1]*

[1] Institut Cochin, INSERM U1016/CNRS UMR 8104, Université de Paris, Paris, France.

[2] Inserm U1037, CNRS U5071, Université Toulouse III, Centre de Recherches en Cancérologie de Toulouse (CRCT), Toulouse cedex, France.[3]

[3] ENS Paris-Saclay, Université Paris-Saclay, CNRS UMR8113, IDA FR3242, Laboratory of Biology and Applied Pharmacology (LBPA), Gif-sur-Yvette, France.

* Corresponding author

E-mail : thierry.tchenio@inserm.fr;

Running Title: Beclin-1 and Cyclin A2 determine kinetics of clinical metastatic recurrence

Keywords: metastase, cancer cell persistence, minimal residual disease, clonogenicity, drug resistance, Beclin-1, Cyclin A2, prostate adenocarcinoma, pancreas adenocarcinoma.

Conflict-of-interest statement: The authors have declared that no conflict of interest exists.

Abstract

Self-sustained quiescence (SSQ) has been characterized as a stable but reversible non-proliferative cellular state that limits the cloning of cultured cancer cells. By developing refined clonogenic assays, we showed here that cancer cells in SSQ can be selected with anticancer agents and that culture at low cell density induced SSQ in pancreas and prostate adenocarcinoma cells. Pre-culture of cells in 3D or their pretreatment with pharmacological inhibitors of mechanistic target of rapamycin (mTOR) synergize with low cell density for induction of SSQ in a Beclin-1-dependent manner. Dissociated pancreatic adenocarcinoma (PAAD) cells rendered defective for SSQ by down-regulating Beclin-1 expression exhibit higher tumor growth rate when injected subcutaneously into mice. Conversely, dissociated PAAD cells in SSQ promote the formation of small indolent tumors that eventually transitioned to a rapid growth phase. *Ex vivo* clonogenic assays showed that up to 40% of clonogenic cancer cells enzymatically dissociated from resected growing mouse tumors could enter SSQ, suggesting that SSQ could significantly impact the proliferation of cancer cells naturally dispersed from tumors. Remarkably, the kinetics of clinical metastatic recurrence in 124 patients with pancreatic adenocarcinoma included in the TGCA-PAAD project could be predicted from the mRNA levels of Beclin-1 and Cyclin-A2, a marker of both cell proliferation and mTOR complex 1 activity, in their primary tumor. Overall, our data show that SSQ is likely to promote the late development of clinical metastases and provide a rationale for a better selection of patients eligible for intensive adjuvant chemotherapy. Additionally, they suggest that identifying new agents targeting cancer cells in SSQ could help improve patient survival.

Significance: This study reveals that a particular state of cancer cell quiescence could largely determine delayed clinical metastasis, challenging current models of cancer cell persistence and offering new avenues for improving adjuvant chemotherapy.

Introduction

Metastases are the leading cause of cancer-related morbidity and mortality and account for more than 80% of cancer deaths. Metastasis involves cancer cells, isolated or in clusters of a few cells, that are disseminated from the primary tumors to distant sites by lymphatic or hematogenous routes. Metastases development is an inefficient process. In experimental models, only a small fraction of cancer cells that have extravasated in the parenchyma of a distant organ begins to proliferate to form micro-metastases, with most of cancer cells entering into a non-growing state called dormant [1-3]. Additionally, only a small subset of micro-metastases continue to grow to form macroscopic tumors [1-3] and the growth of small macroscopic tumors into larger tumors is also limited [4, 5]. Unfortunately, the mechanisms that limit development of metastases are also probably involved in the persistence of cancer cells in patients in complete remission, and are a cause of the late development of metastases [5-7].

Since a metastase is basically a clonal cell population resulting from the proliferation of a single disseminated cancer cell, we have undertaken studies on the factors limiting the cloning of cancer cells in culture in order to better understand the factors regulating the development of metastases. This led us to discover that the ability of prostate adenocarcinoma (PA) cells to proliferate at low cell density to form a cell clone can be severely limited by a phenomenon we initially called dormancy [8, 9] by analogy with the phenomenon of cancer cell dormancy [5]), then renamed Self-Sustained Quiescence (SSQ) [10] to highlight its cell-autonomous feature. Indeed, PA cells can be induced to enter a G0/G1 growth-arrested state that, once established, maintains itself at low cell density despite the return of cells to growth-permissive conditions. We showed that this self-sustained growth arrest involves a stable decrease of the redox

potential of cellular thiols and is further stabilized by BMP signaling pathways [10]. Accordingly, cells in SSQ can be switched to a proliferating state when treated with SSQ inhibitors (SSQi) consisting of a reduced thiol (such as dithiothreitol, glutathione or N-acetylcysteine) and/or an inhibitor of BMP signaling (such as K02288; see also the Methods section for more details) [8-10]. Additionally, SSQ can be destabilized by autocrine factors of less than 2 kDa produced by most types of cancer cells grown in 2D culture (see S1 Fig in [9] and unpublished data). The self-maintenance property of SSQ is remarkable compared to other models of cancer cell dormancy that in most cases involved mechanisms that are non-cell-autonomous in accordance with the "seed and soil" model. This raises the issue of the biological relevance of SSQ in the regulation of tumor development. Here we showed that PA and pancreatic ductal adenocarcinoma (PADC) cells in SSQ or competent for SSQ can be selected with anticancer agents after subculturing cells at low cell density. This allowed the characterization of factors modulating induction of SSQ and the isolation of PDAC cell populations highly enriched in SSQ that we used for *in vivo* studies. We then applied the results obtained to the analysis of metastasis in pancreas adenocarcinoma (PAAD) patients.

Results

Characterization of clonogenic cancer cells in SSQ through their selection with anticancer agents at low cell density.

We hypothesized that anticancer agents that preferentially target proliferative cells could allow to select cells in SSQ. We used KC-DT66066 cells, derived from a pancreas ductal adenocarcinoma (PDAC) developed in a genetically engineered LSL-Kras$^{G12D/+}$, Pdx1-Cre mouse model of spontaneous PDAC [11, 12] and routinely passaged at medium/high cell density in 2D-culture plates. When these cells were plated at low cell density in regular growth

medium, they exhibited high cloning efficiency (CE=48 ± 14 % of seeded cells grew to form cell clones; mean ± sd, n=24; see the none→ none clonogenic assay in Fig 1A-B) that was slightly increased by addition of SSQi (59 ± 17 %; see the none→ SSQi clonogenic assay in Fig 1A-B). To test for the selection of cancer cells in SSQ with gemcitabine, KC-DT66066 cells were plated at low density in regular growth medium and cultured for 3 days before applying gemcitabine selection for 4 days. When cells were washed and returned to their regular growth medium, very few, if any, growing cell clones were detected after 10-12 days, even after microscopic examination (see gem d3 → none in Fig 1A-B). However, when cells were returned to regular growth medium supplemented with SSQi after gemcitabine selection, growing cell clones were recovered at an averaged frequency of 1.5% of seeded cells (see gem d3→ SSQi in Fig 1A-B). This showed that non-growing cells that had survived to gemcitabine treatment were in SSQ since they switched to a proliferative state only after adding SSQi. Interestingly, the recovery of growing cell clones was reduced to background (<0.4%) if gemcitabine was added immediately after cell seeding (see gem d0→ SSQi in Fig 1A-B). This indicated that most cells from 2D-cultures entered SSQ only after plating at low cell density.

As this induction of SSQ could be counteracted by growth factors that promote cell proliferation, we tested whether low fetal calf serum concentration in growth medium (low FCS) could facilitate SSQ induction after plating at low cell density. After plating for 3 days at low cell density in low FCS, spontaneous cloning efficiency (CE) decreased to 13% of seeded cells but was increased twofold by adding SSQi (see low FCS in Fig 1A-B). This suggests that clonogenic cancer cells that survive to culture at low cell density in low serum were more susceptible to the clonal cell growth promoting effect of SSQi. Correspondingly, frequency of cancer cells in SSQ selected by gemcitabine increased to 3.4% of seeded cells under these conditions, showing that reduced serum concentration synergized with low cell density to induce SSQ (see low FCS→ gem→ SSQi in Fig 1A-C).

Of note, the addition of SSQi could be delayed for at least 3 days after completion of gemcitabine selection with no significant decrease of cell clone recovery, showing that SSQi did not rescue cancer cells undergoing a delayed cell death phenomenon that might have been induced by gemcitabine treatment (S1A Fig). In fact, the addition of SSQi at the same time as gemcitabine completely blunted the subsequent recovery of growing cell clones (see low FCS→ gem + SSQi→ SSQi in Fig 1A-B). This showed that SSQi sensitized cells to gemcitabine, as expected if the only action of SSQi is to promote the switch from SSQ to proliferative state. These observations were generalized to others pancreas and prostate cancer cell lines (S1B, D-E Fig) and anticancer drugs exhibiting a strong and selective toxicity to proliferating cancer cells (S1D-E Fig). In the remainder of this article, the clonogenic assay gem d0-→ SSQi was used to measure the relative frequencies of cells already in SSQ in the cell populations studied (Fig 1D). The relative frequency of clonogenic cancer cell in SSQ measured by clonogenic assays with delayed selection by gemcitabine (gem d3→ SSQi or low FCS→ gem d3→ SSQi) corresponds to the sum of the relative frequency of cancer cells already in SSQ in the cell population studied and the relative frequency of their induction by low cell density and low serum (Fig 1D).

SSQ is promoted by 3D cell culture and treatment with pharmacological inhibitors of mTOR.

We observed that KC-A338 cells entered SSQ at high frequency in 2D culture (S1B Fig), which correlated with their ability to spontaneously form transformed foci that eventually detached from the bottom of the culture dish to form compact tumor spheroid-like structures (S1C Fig). This led us to investigate whether 3D culture could promote SSQ. 3D culture of KC-DT66066 cells on cell-surface-repellent plates in their regular growth medium resulted in the formation

of small, non-growing and loosely attached cell aggregates (Fig 2A-B). However, when growth medium was supplemented with conditioned medium (CM) harvested from senescent mouse fibroblasts cultures that produce numerous growth factors and cytokines [13], compact growing spheroids were obtained (Fig 2A-B). Analysis of the expression of stemness markers by RT-qPCR showed that non-growing cell aggregates overexpressed *Aldh1* while growing spheroids overexpressed *Lgr5* (Fig 2C and see S1 Data for the full list of genes tested). Interestingly, the gem d0 → SSQi clonogenic assay showed that 6-7 % of clonogenic cancer cells had entered SSQ during 3D culture both as non-growing cell aggregates or growing spheroids (Fig 2D). Moreover, cells from 3D culture exhibited an increased rate of SSQ induction after plating at low density in reduced serum (compare low FCS→ gem → SSQi between 2D control, 3D and 3D+CM in Fig 2D). In an attempt to understand why SSQ was promoted by 3D cell culture, we examined the possible role of autophagy since cell detachment from the extracellular matrix can induce autophagy [14]. Therefore, we used the autophagy gene reporter GFP-LC3-RFP-LC3ΔG [15] to measure the autophagic flux and observed that it was stably enhanced in 3D cultured cells (Fig 2E-G). This led us to examine whether stimulation of autophagy in 2D cell culture could promote SSQ. Accordingly, cells grown at medium cell density in standard culture plates were pretreated for 1 day with Torin1 [16], a standard inhibitor of mTOR that strongly induces autophagy [15], then harvested and seeded at low cell density to test for SSQ induction as described in Fig 1A. Torin1 pretreatment strongly increased the induction of SSQ by plating cells at low density in reduced serum (compare low FCS→ gem → SSQi between pretreated and non-pretreated cells in Fig 2D). Moreover, the gem d0-→ SSQi clonogenic assay indicated that at least 2 % of clonogenic cancer cells were induced to enter SSQ before plating cells at low density. These data were confirmed using rapamycin, the canonical mTOR inhibitor and both Torin1 and rapamycin also increased SSQ in human prostate adenocarcinoma cell lines

(S2A-B Fig). Taken together, these results showed that inhibition of mTOR signaling pathways was sufficient to strongly promote the induction of SSQ in cancer cells.

Beclin-1 expression is required for SSQ induction in an autophagy-independent manner.

To further investigate the possible role of autophagy in regulating SSQ induction, we focused on Beclin-1 (Becn1) that promotes autophagosomal membrane nucleation [17]. Beclin-1 is released from the cytoskeleton upon mTOR Complex 1 (mTORC1) inhibition and is also required for induction of autophagy by cell detachment from extracellular matrix [14, 18, 19]. We generated 3 independent cell populations transduced with a *Becn1*-targeting lentiviral shRNA that exhibited a 90% reduction in *Becn1* mRNA level, compared to cell populations transduced with a *gfp*-targeting control lentiviral vector (KCsh*Becn1* and KCsh*gfp* cell populations, respectively; data not shown and see below). Clonogenic assays as performed in Fig 1 showed that induction of SSQ was significantly decreased by *Becn1* downregulation (Fig 3A). Furthermore, this could not be alleviated by Torin1 pre-treatment of cancer cells, which increased the frequencies of cells in SSQ only in control cell populations (KCsh*gfp*, Fig 3B).

Western Blot analysis showed that KCsh*Becn1* cell populations displayed a 10-fold decrease of Beclin-1 (Fig 3C). Phosphorylation of p70S6 kinase and 4EBP1, two downstream targets of mTOR complex 1 (mTORC1) was strongly inhibited by Torin1 treatment in both control and KC*shBecn1* populations (Fig 3C). Akt1 phosphorylation at serine 473 was less affected by Torin-1 treatment (Fig 3C), consistent with phosphorylation of this site by several kinases in addition of mTOR complex 2 [20]. Interestingly, the expression of LC3-II (a cleavage product of LC3-I (Atg8) and a marker of autophagosomes formation) showed no significant difference between control and KCsh*becn1* cells under basal conditions or after treatment with bafilomycin A1 (an autophagy inhibitor that induced an accumulation of LC3-II [21]; Fig 3C).

Additionally, the level of Sqstm1, a protein degraded by autophagy, was barely detectable under basal conditions in both control and KCsh*becn1* cells, but was increased by bafilomycin A1 treatment (although to a lesser extent in KCsh*becn1* cells; Fig 3C). This suggests that autophagy was barely affected by Beclin-1 downregulation, which was confirmed by comparing autophagic flux in several independent KCsh*gfp* and KCsh*Becn1* cell populations (Fig 3D). Thus, Torin1 treatment could promote SSQ through Beclin1-dependent mechanisms that are unrelated to autophagy. This was further supported by experiments in which inhibition of autophagy with bafilomycin A1 (which affects autophagy downstream of Beclin-1 activation) did not have a significant impact on the induction of SSQ by Torin1 in pancreas or prostate adenocarcinoma cells (S2 D-E Fig). The dependence of SSQ on Beclin-1 was also verified with KC-A338 cells in which downregulation of *Becn1* mRNA levels by fourfold resulted in a 2.7 fold reduction of cancer cells in SSQ that could be selected with the gem d0 clonogenic assay (S2C Fig).

SSQ regulates tumor growth in vivo in mice.

When 10^6 carefully dissociated KC-DT66066 cells harvested from growing cultures were subcutaneously injected in allogenic C57Bl/6 mice, they gave rise to fast-growing tumors that began to regress after approximately one week due to immune rejection of cancer cells. Even during this short period of growth, we observed a higher tumor growth rate with Beclin-1 deficient cell population (KCsh*Becn1*) compared to the control (KCsh*gfp*) (S3A Fig). Interestingly, we found that treatment with a high dose of gemcitabine on day 4 after cell injection increased KC cell tumorigenicity, possibly by depressing the immune response (data not shown and see [22]). Under these conditions, the higher growth rate of KCsh*Becn1* cells was confirmed because KCsh*becn1* cells, but not the control population, were able to out-compete the immune response (S3B Fig). Considering that KCsh*becn1* and KCsh*gfp* cell

populations exhibited the same growth rate in 2D culture at medium cell density (S3C Fig) and the same percentage of clonogenic cells (compare none→ SSQi in Fig 3A and 3B), these experiments suggested that a significant fraction of control cells could enter SSQ *in vivo*, resulting in a lower tumor growth rate. Of note, they also showed that KC-DT66066 cells exhibit high resistance to gemcitabine *in vivo*, which is not dependent on Beclin-1 expression. To further investigate the role of SSQ in regulating tumor growth, we analyzed the tumorigenicity of KC-DT66066 cells in immunodeficient NOD-SCID mice. As few as 100 dissociated cells harvested from exponentially growing cell cultures gave rise to rapidly growing tumors in these hosts (S3D Fig). To test the contribution of cells in SSQ, we subcutaneously injected 4 mice with 500 cells obtained from exponentially-growing culture (which were refer to as the Exp group that additionally included 2 mice previously injected with 100 proliferating cells, n=6) and 8 mice with 500 cells enriched for SSQ by Torin 1 treatment and gemcitabine selection in cell culture (Fig 4A and Methods). Mice injected with cells enriched for SSQ were further divided into 2 groups that were treated with saline (Ssq/none group, n=4) and gemcitabine on the 4th and 11th day after cell injection (Ssq/gem group, n=4; Fig 4A and Methods). Gemcitabine treatment was performed with the aim of counter selecting cancer cells that started to proliferate shortly after cell injection to further enrich the injected cells for SSQ cells *in vivo*. A distinct palpable tumor mass (≈10 mm^3) could be detected in all the mice in the Exp and Ssq/none groups and in 3 of the 4 mice in the Ssq/gem group around the 30th day after cell injection (Fig 4B-C). These results indicated that the initial phase of tumor growth was not significantly affected by the state of the cells prior to injection or by treatment with gemcitabine. However, subsequent tumor growth differed in the groups of mice injected with SSQ cells. While all tumors in mice of the Exp group grew vigorously and rapidly reached a tumor volume of 100 mm^3 approximately one week later (36.7 ± 3.9 days, mean ± s.d., n=6), 2 of the 4 tumors in the mice of the SSQ/none group thereafter grew very slowly and reached

100 mm^3 only on the 67th day after cell injection. This corresponded to a difference with the mean tumor growth time of the Exp group of more than 7 times the standard deviation of tumor growth times in the Exp group (Fig 4B and 4D). Such a large difference makes it unlikely the occurrence of slow-growing tumors in the Exp group if one assumes a Gaussian distribution of tumor growth rates in this group. Additionally, a third mouse in the Ssq/none group developed a tumor that quickly reached 200 mm^3 on the day 37, but then ceased to grow until sacrifice of this mouse on day 47 due to skin ulceration (Fig 4B). The proportions of slow-growing tumors in the Exp and Ssq/none groups (0/6 *vs* 3/4) were found statistically different as calculated with a Fisher's exact probability test (p=0.033). This confirmed that formation of tumors with a slow-growing phenotype is promoted by the injection of cancer cells in SSQ. Similar observations were made with mice in the Ssq/gem group (3 of 4 mice also developed slow-growing tumors), but, additionally, one mouse also showed delayed formation of a palpable tumor (it was detected on day 65 after cell inoculation; Fig 4B-D). This showed that cancer cells in SSQ promoted the formation of indolent tumors at high frequency and that SSQ could also impede the early phase of tumor growth. Nonetheless, all of the indolent tumors, including the one that had been indolent for two months, eventually transitioned to a rapidly growing phase, consistent with our concept of a stable but reversible quiescence (Fig 4B). Genes expression profiling of growing tumors by RT-qPCR analysis did not reveal any significant difference associated with the status of the injected cells (correlation coefficient r>0.99, n = 17 genes analyzed, p <0.0001; S3E Fig and S1 file). Interestingly, in comparison with exponentially growing KC-DT66066 cells in 2D-cultures, all growing tumors displayed an increased expression level of the *Lgr5* stemness marker, as observed for cells growing in spheroids (compare Fig 2C and S3E Fig). This analogy between spheroids and tumors was further supported by analysis of the clonogenicity of dissociated tumor cells, as previously done for spheroids (Fig 2D, 4E and see Methods). This not only confirmed the presence within the

tumors of significant populations of cells in SSQ (18.7± 8.2% of clonogenic tumor cells selected with the gem d0 clonogenic assay, mean ± sd, n=5; Fig 4F), but also revealed that clonogenic tumor cells were prone to enter SSQ (27.3 ± 11.4% of clonogenic tumor cells selected with the low FCS→ gem→ SSQi clonogenic assay, mean ± sd; n=5; Fig 4F). Interestingly, in tumors that grew in allogenic C57Bl/6 mice injected with 10^6 proliferating KC-DT66066 cells, clonogenic assays also revealed cancer cells in SSQ or prone to enter SSQ after seeding at low cell density under low serum, but at lower frequencies (1.3 ± 0.7% and 3.0 ± 1.7% of clonogenic cells, respectively, mean ± sd, n=5). However, these frequencies significantly increased when C57Bl/6 mice were treated with cyclosporine, an immunosuppressive agent (4.50±1.1% and 14.8±4.9% of clonogenic cells, respectively; n=4, $p<0.002$; see Methods for more details), suggesting that immune response could modulate frequency of SSQ cells in tumors.

High Beclin-1 level and low mTOR activity in the primary tumor of PAAD patients is predictive of late metastatic recurrence.

Based on our results in mice, primary tumors with a relatively low level of Beclin-1 expression should release cancer cells that are not prone to enter SSQ, and thus cause a lower rate of late metastasis if SSQ constitutes the only mechanism controlling delayed metastases development in pancreatic adenocarcinoma (PAAD). Analysis of PAAD patient records downloaded from the Genomic Data Commons website (see Methods) showed that the rate of distant metastases in the first 360 days after initial treatment did not differ significantly between cohorts of patients with low and high level of Beclin-1 transcripts in their primary tumors (Fig 5A). However, beyond 360 days, a low level of Beclin-1 transcripts in the primary tumor was associated with a decreased rate of distant metastases (Fig 5B and see the Methods section for the cutoff value of *BECN1* mRNA levels used throughout this study). This remained true when we restricted

the analysis to patients with a similar T3N1M0/Mx clinical grade (S4A-B Fig), suggesting that Beclin-1 expression level is a predictive factor of late metastasis independent of TNM grade. To further establish the biological relevance of a 360-day cutoff for classifying patients as developing early or late metastases, we compared the primary tumors transcriptomes of patients with distant metastasis-free survival less than and greater than 360 days by Gene Set Enrichment Analysis (GSEA). GSEA recovered only 8 statistically significant genes sets with a false discovery rate (FDR) $q<0.05$. They showed that primary tumors from patients with a distant-metastasis-free survival inferior to 360 days were enriched for genes regulated by MYC transcription factor, mTORC1 signaling and the unfolded protein response (Fig 5C and see S4C Fig for others miscellaneous gene sets). This suggested that a distinguishing feature of tumors from patients with a distant metastasis-free survival inferior to 360 days might be enrichment in proliferating cells (enhanced MYC activity) that exhibited higher protein synthesis (enhanced mTORC1 signaling) associated with endoreticulum stress (enhanced unfolded protein response). Thus, we analyzed distant metastasis-free survival of PAAD patients according to the relative level of Cyclin A2 (*CCNA2*, a marker of cell proliferation) in their primary tumor since mTORC1 activity seemed to be associated to tumor cell proliferation in the primary tumors. A high level of Cyclin A2 transcript was found to be a very strong predictor of early metastasis with a median survival time of 291 days *versus* 763 days in the cohort of patients with a low level of Cyclin A2 transcript (Fig 6A and see the Methods section for the cutoff value of CCNA2 mRNA levels used throughout this study**)** and this was independent of TNM grade (S4D Fig). Independence was also confirmed by multivariate Cox regression analysis (data not shown). GSEA showed that primary tumors with a high level of Cyclin A2 transcripts were highly enriched for classical hallmarks of cell proliferation, but also enhanced mTORC1 signaling and unfolded protein response (Fig 6B and S4E), as anticipated above. The strong correlation between the transcript levels of Cyclin A2 and of markers of mTORC1 activity in

the primary tumors of PAAD patients were confirmed by hierarchical gene clustering (Fig 6C). Interestingly, this analysis also showed that levels of Beclin-1 and Cyclin A2 transcripts (as well as mTORC1 activity marker genes) were positively correlated with levels of cancer cell markers but not mesenchymal, endothelial or immune cell markers (Fig 6C and S4F). This suggested that transcript levels of Beclin-1 and Cyclin A2 in the primary tumors were mainly determined by cancer cells.

The combination of Beclin-1 and Cyclin A2 markers showed that all metastatic events within the first 360 days after initial treatment were associated with tumors with either high Cyclin A2 or both low Cyclin A2 and low Beclin-1 expression (Fig 6D). Remarkably, patients whose tumors exhibited both low Cyclin A2 and high Beclin-1 expression did not develop metastases within the first 360 days after initial treatment (Fig 6D). However, after 360 days, patients with both low Cyclin A2 and high Beclin-1 expression exhibited a higher rate of distant metastasis compared to patients with both low Cyclin A2 and low Beclin-1 expression in their primary tumors (Fig 6E). Taken together, this strongly suggests that Beclin-1 abundance and mTORC1 activity in the primary tumor of PAAD patients determine the kinetics of occurrence of clinical metastases. This was further confirmed by analyzing the statistics of relative proportions of early and late clinical metastasis (before and after 360 days) according to tumor phenotype of patients with a T3N1M0/x clinical grade (Table 1). This showed that late clinical metastasis was mainly associated to the *CCNA2*^{low} *BECN1*^{high} primary tumor phenotype and early clinical metastasis to the *CCNA2h*^{igh} and the *CCNA2l*^{ow} *BECN1*^{low} primary tumor phenotypes.

Table 1: **Early and late (before and after 360 days, respectively) distant metastases events recorded in T3N1M0/x PAAD patients according to their primary tumor phenotype.**

primary tumor phenotype (number of patients)	SSQ competence	Early metastases events[a]	Late metastases events[b]	Fisher's exact test[c]
CCNA2^{high} **(n=20)**	low	8	2	0.0007
CCNA2^{low} BECN1^{low} **(n=41)**	low	10	4	0.0016
CCNA2^{low} BECN1^{high} **(n=18)**	high	0	9	-

[a] within 360 days of initial treatment.
[b] beyond 360 days after initial treatment
[c] Statistical significance of the difference in the repartition of early and late metastases events compared to the cohort of patients with a *CCNA2*^{low} *BECN1*^{high} tumor phenotype.

Discussion

We showed here that cancer cells in SSQ can be selected with anticancer agents including gemcitabine, vincristine, nocodazole, doxorubicin, oxaliplatin and taxol *in vitro* (Fig 1, S1D-E and data not shown) and possibly also *in vivo* (Fig 4A-B). This suggests that SSQ could promote the persistence of disseminated cancer cells after adjuvant chemotherapies. Analysis of the mechanisms of SSQ induction showed that culture at low cell density induces SSQ in prostatic and pancreatic adenocarcinoma cells (Fig 1B and data not shown). By investigating why SSQ is also induced at high cell density in non-growing cell aggregates or in growing cancer cell spheroids generated in 3D culture (Fig 2D), we found that it is induced by mTOR inhibition. Indeed, pretreatment of growing cancer cells cultured in 2D at medium cell density with rapamycin or Torin1, two standard pharmacological inhibitors of mTOR activity, is sufficient

to induce SSQ and also synergizes with low cell density for SSQ induction (Fig 2H and S2A-B). As cell proliferation depends on mTOR activity [24-26], this implies that proliferating cells are not prone to enter SSQ, in agreement with our finding that exponentially growing cell cultures in 2D exhibited low frequency of cancer cells already in SSQ and are modestly induced to enter SSQ after seeding at low cell density (Fig 1B). Inversely, in 3D cultures, high levels of autophagy indicate that mTOR activity was downregulated in a large fraction of cells since mTOR activity inhibits autophagy. An unexpected result is our finding that induction of SSQ requires Beclin-1 expression but was independent from autophagy. Indeed, downregulation of Beclin-1 inhibits induction of SSQ but not of autophagy (Fig 3) and inhibition of autophagy with bafilomycin A1 does not prevent SSQ induction by Torin1 (S2C Fig). This suggests that Beclin-1 regulates SSQ through autophagy-independent pathways. Several publications have already reported autophagy-independent roles for Beclin-1. In particular, Beclin-1 regulates degradation of cell membrane receptors for growth factors and transferrin through the control of endolysosomal trafficking [17, 27-29]. It can also inhibit the System Xc^- cystine/glutamate antiporter involved in cystine uptake, thus impacting cellular thiol redox potential [30] and Stat3 signaling pathway [31]. These actions of Beclin-1 could contribute to two main features of cancer cells in SSQ which are the absence of proliferating response to stimulation by external growth factors and a decrease in the redox potential of cellular thiols. Considering that mTOR activity is regulated by nutrient depletion, cellular thiol redox potential and growth factor signaling [32-39], activation of Beclin-1 through inhibition of mTOR activity could therefore promote the establishment of a self-sustained inhibitory loop maintaining a low mTOR activity (Fig 7). As mTOR also directly control cell proliferation through its regulation of c-Myc activity and Cyclin D accumulation [24-26], our data point towards a central role of mTOR downregulation and Beclin-1 activation in the induction and maintenance of self-sustained quiescence (Fig 7).

Another finding from our work is that when dissociated PADC cells in SSQ were injected into mice, they promoted the delayed formation of a palpable tumor in one case, as expected for the dormant phenotype of cancer cells in SSQ *in vitro*, but also, quite unexpectedly, the formation of small, slow-growing (indolent) tumors in most cases (Fig 4). Our data suggest that SSQ can directly regulate tumor cell growth and thus tumor indolence when tumor is composed of a high percentage of SSQ-competent cells. Indeed, we observed that the mouse tumor microenvironment promotes SSQ. A large fraction of clonogenic cancer cells dissociated from resected tumors were found to be in SSQ or prone to enter SSQ after cell plating at low cell density, this even in tumors resulting from the injection of exponentially growing cancer cells exhibiting a low frequency of cells in SSQ or competent for SSQ (see the Result section and also compare data in Fig 1 and 4E after their normalization by the frequencies of clonogenic cells determined by the none → SSQi clonogenic assays). This SSQ-promoting effect of tumor microenvironment could explain why tumors generated by the injection of a large number of exponentially growing cancer cells rapidly exhibit a higher growth rate when these cells have been made defective for SSQ by Beclin-1 downregulation whereas downregulation of Beclin-1 has no effect on proliferation of cells cultured at medium cell density (S3A-C Fig). Accordingly, a plausible mechanism of long-term tumor indolence is the maintenance of a high percentage of cancer cells in SSQ through the continuous induction of SSQ by tumor microenvironment. Breaking this steady state through the rapid outgrowth of cancer cells refractory to SSQ induction or changes in the tumor microenvironment would resume a high tumor growth rate. Taken together, these results challenges models of tumor dormancy that posit a dynamic balance between cancer cell proliferation and cell death caused by antitumor immunity and insufficient tumor vascularization [41].

Our analysis of the relationship between metastasis in PAAD patients and gene expression in their primary tumor showed that tumors that are expected to contain and therefore disseminate

clonogenic cancer cells that are not prone to enter SSQ mainly give rise to early clinical metastasis whereas those that are likely to disseminate cancer cells in SSQ or poised to enter SSQ give rise to late clinical metastasis (Figs 5-6 and Table 1). Indeed, tumors expressing a higher level of Cyclin A2, a marker of cell proliferation, also exhibit higher mTORC1 activity (Fig 6B-C), which inhibits induction of SSQ (see discussion above and Fig 7). Similarly, a low level of Beclin-1 transcripts was found to decrease the ability to enter SSQ (Fig 3), even in growth-arrested cells cultured in 3D (data not shown). Conversely, a high level of Beclin-1 expression, when combined with low mTORC1 activity associated with low Cyclin A2 expression, is expected to promote entry in SSQ (Fig 3). Of note, Cyclin A2 mRNA, in addition to being a marker of cell proliferation, is also a hallmark of c-Myc activity (it is the highest ranked gene in the GSEA analyses showing enrichment for c-Myc targets in Fig 6B and the eighteenth ranked gene in Fig 5C). Correlatively, one of the most distinctive features of patients with early metastasis (EM-patients) is an enrichment of their primary tumor with cellular markers for c-Myc activity (Fig 5C and 6B). This suggests that c-Myc activity could be a better hallmark of mTORC1 activity in primary tumors activity rather than cell proliferation, which is consistent with c-Myc regulation by mTORC1 signaling via Beclin-1-dependent and independent pathways [24, 42] and a high correlation between mRNA levels of Cyclin A2 and markers of mTORC1 activity (Fig 6C).

Beclin-1 is often considered a haplo-insufficient tumor suppressor gene since Beclin-1 can inhibit tumorigenesis [43] and an allele of this gene is frequently deleted in advanced cancers [44]. A high Beclin-1 expression level in the primary tumor of PAAD patients was successively associated with a low rate of metastasis in one study and then with a high rate of metastasis in another [45, 46]. This paradox could partly result from the short follow-up of patients with high Beclin-1 in the first study, since we found that high Beclin-1 expression shows a trend to promote a lower rate of early metastasis (Fig 5A). However, it should be noted that our data

support the idea that Beclin-1, combined with mTORC1 activity, primarily determines the kinetics of metastases development and not the overall rate of metastasis.

A possible direct clinical application of our results is a better selection of patients eligible for early and aggressive adjuvant chemotherapy. Indeed, our results suggest that patients with a primary tumor associated to dispersion of cancer cells not entering SSQ could benefit from aggressive chemotherapy since their dispersed cancer cells are expected to be sensitive to anticancer agents. It is crucial that adjuvant chemotherapy begins as early as possible since cancer cells grown in tumor masses gained additional mechanisms of resistance to anticancer agents compared to dispersed cancer cells, including the possible *de novo* generation of cancer cells in SSQ within tumor microenvironment. Patients with dispersed cancer cells only in SSQ (patients with a primary tumor phenotype associated to late metastasis or treated once by an aggressive adjuvant chemotherapy) are unlikely to respond well to chemotherapy since these cancer cells are resistant to anticancer agents even when they are dispersed. Therefore, the development of new agents targeting cancer cells in SSQ seems essential. Complete elimination of dispersed cancer cells in SSQ may require the identification of agents that are effective in stably reversing SSQ *in vivo* to restore cancer cell susceptibility to chemotherapy or in directly killing cancer cells in SSQ.

Materials and Methods

Cells: All cells were cultured under 5% CO_2 at 37 °C in Dulbecco's Modified Eagle's Medium-high glucose (4.5 $g.L^{-1}$ glucose, glutamax 1X; #D0819 Sigma Aldrich) supplemented with fetal calf serum (10% of DMEM volume; #10270-106; various lots; GIBCO, Life Technologies), pyruvate 1 mM (#CSTVAT00-0U from EUROBIO), penicillin/streptomycin 1X (#15140-122 from GIBCO), to which distilled water was added (17.6% of DMEM volume) to make it isotonic (isoDMEM-FCS). Final fetal calf serum (FCS) concentration was 7.9% in growth

medium and was decreased to 1.9% for low FCS condition by dilution with isoDMEM. For subculturing, cells were harvested after 5 min treatment with 0.25% trypsin-EDTA (#25200-056 from Gibco) supplemented with 1 mM pyruvate (Tryp-EDTA-Pyr), dissociated by pipetting, counted using a hemocytometer if necessary and inoculated at a dilute density. KC (-DT66066, -A338, and -A419) and KPC-A219 are independent cell lines derived from pancreas ductal adenocarcinoma (PDAC) developed in genetically engineered LSL-*Kras*$^{G12D/+}$, Pdx1-*Cre* (KC) and LSL-*Trp53*$^{R172H/+}$, LSL-*Kras*$^{G12D/+}$, Pdx1-Cre (KPC) mouse models of spontaneous PDAC, respectively [11, 12]. All KC and KPC-A219 cells were derived in J. Guillermet laboratory under a genetic C57Bl/6 x CD1 and C57Bl/6 x CD1 x 129 genetic background, respectively, and were authenticated by PCR. Human LNCa* and LNCaP C4-2 (RRID:CVCL_4782) prostate adenocarcinoma were characterized previously [10]. Cells were found to be free of mycoplasma by a PCR test carried out on their supernatant.

Reagents: anti-Beclin-1 (clone D40C5, #3495S), anti-GAPDH (clone D16H11, #5174), anti-4E-BP1 (clone53H11, #9644), anti-phospho-4E-BP1 (Thr37/46; clone236B4, #2855), anti p70 S6 kinase (clone 49D7, #2708), anti-phospho-p70 S6 kinase (Thr389) (clone 108D2, #9234) and anti-LC3A/B (clone D3U4C, #12741) were rabbit monoclonal antibodies from Cell Signaling Technology. Anti-Akt (#9272) and anti-phospho-Akt (S473; #9271) were rabbit polyclonal antibodies from Cell Signaling Technology. Anti-SQSTM1 (#GT239) was a mouse monoclonal antibody from Invitrogen. Secondary HRP-linked anti mouse IgG (7#076S) and anti rabbit IgG (#7074S) were from Cell Signaling Technology. K02288 (#AB-M2789-10MG), Torin1 (#F6100-UBP) and rapamycin (#AB-M1768-25MG) from AbMole BioScience (USA), N-acetyl-L-cysteine (#A7250) from Sigma-Aldrich, Nocodazole (#F6120-UBP) was from UPBIO. Gemcitabine chlorhydrate and Cyclosporin A were from Sandoz (France) and Vincristine Sulfate from Hospira (France). Lipofectamine 3000 kit (#L3000-00) was from

Invitrogen. LightCycler 480 SYBR Green I Master kit (#04707516001) was from Roche Diagnostics, USA)

Clonogenic assays: 2D-cultured murine pancreas and human prostate C4-2 cells were seeded at 10^3 cells per 60 mm diameter tissue culture-treated polystyrene dish (#430169, Corning, NY, USA) for selection of SSQ cells with anticancer agents, otherwise at 10^2 cells per dish and cultured as indicated. Human LNCaP* cells were seeded at 5000 cells per 6 cm diameter dish and cultured as indicated. To test the cloning efficiency (CE) of cells from 3D-cultures, cells were harvested, washed one time with Tryp-EDTA-Pyr and then dissociated by incubation for 20 minutes in Tryp-EDTA-Pyr at 37°C with regular pipetting. Complete growth medium was added and cells were filtered through a 70µm Cell Strainer (Falcon, Corning), washed once with complete growth medium, counted and plated at low cell density as needed. For the CE tumor cell assay, tumors were minced and cells dissociated using the same protocol as for spheroids. Only cells larger than 20 µm were counted with a hemocytometer to calculate cell dilutions for clonogenic assays (cells smaller than 20 µM were not clonogenic). In 7 of the 8 tumors analyzed, more than 90% of the clonogenic tumor cells were KC-DT66066 cells that generated easily recognizable dense and rapidly growing cell clones. In an tumor from the Ssq/none group that was not included in CE analysis, long-lived fibroblast cells constituted more than 90% of the clonogenic tumor cells and generated only sparse, slow-growing cell clones. Cell clones were fixed in 50% ethanol and 10% acetic acid, stained with crystal Violet and counted manually (clones with a diameter > 0.5 mm). Cloning efficiency (CE) was calculated as the ratio of the number of cell clones to that of seeded cells. Cloning efficiency in the presence of SSQ inhibitors (SSQi) was used as a measure of the percentage of clonogenic cells. The fraction of cells in SSQ in a cell population was defined as the cloning efficiency of cells from that population in the gem d0→ SSQi clonogenic assay (Fig 1A and main text). SSQi

(NK, GK or GSK) consisted of a reduced thiol (N-Acetylcysteine (NAC or N) or glutathione (G) which could be used with similar efficacy at optimal concentrations) at 1 or 4 mM for murine and human cells, respectively, and of K02288 (K, an inhibitor of BMP signaling) at 100 nM. In murine PDAC cells, K02288 increased by about twofold the recovery of proliferating cell clones from cells in SSQ when NAC concentration was below 0.5 mM but was otherwise unnecessary at 1 mM NAC concentration. Similarly, SB505124 (an inhibitor of TGFβ signaling) was used with K002288 and glutathione (GSK) to reverse SSQ in LNCaP* cells, but its effect was statistically insignificant.

3D culture: Cells were harvested from 2D cultures by treatment with Tryp-EDTA-Pyr, counted and seeded into 24 well-plates (Cellstar, cell-repellent surface, #664970, Greiner Bio-One Gmbh) or into 6 cm dishes (Ultra-Low Attachment, #3261, Corning, NY, USA) at a concentration of 10^4 and 10^5 cells per well or dish, respectively, in regular growth medium and cultured for up to 11 days. Conditioned Medium (CM) was isoDMEM-FCS harvested from primary cultures of fibroblasts derived from 13.5 days C57Bl/6 embryos and made senescent by gemcitabine treatment at 100 ng/ml for 7 days. The CM was filtered through 0.2 µm sized-pore filter and in some experiments concentrated with Amicon Ultra centrifugal filters with a cut-off of 50 kDa or 300 kDa.

Recombinant retrovirus: To downregulate *Beclin-1* expression we used recombinant lentiviral vectors, pLKO1-sh*Becn1*, that encode validated shRNA [47, 48] from the RNAi Consortium (clones TRCN0000087290 and TRCN0000087292 with target sequence 5'-GCGGGAGTATAGTGAGTTTAA-3' and 5'-CGGACAGTTTGGCACAATCAA-3', respectively, distributed by Sigma-Aldrich, Merck, France. pLKO1-sh*gfp* [49] was a gift from David Sabatini (Addgene plasmid # 30323 ; http://n2t.net/addgene:30323 ;

RRID:Addgene_30323) and pMRX-IP-GFP-LC3-RFP-LC3ΔG [15] a gift from Noboru Mizushima (Addgene plasmid # 84572 ; http://n2t.net/addgene:84572 ; RRID:Addgene_84572). To produce retroviral particles, 2 µg of the plasmid carrying the relevant recombinant provirus was co-transfected with 2 µg of plasmid pMD2.G (a kind gift from D. Trono) and 2 µg of plasmid PVPackgagpol (#217566 from Stratagene, La Jolla, CA) or plasmid pCMV-ΔR8.74 (a gift from D. Trono) (for Moloney Murine Leukemia Virus and Human Immunodeficiency Virus derived retroviral backbone, respectively) in 90% confluent HEK293T cells plated in 6 cm diameter dishes using lipofectamine 3000 kit (12 µL of P3000 and 14 µL of Lipofectamine 3000 used). Supernatant were filtered through 0.4 µM filter and used to infect exponentially growing cells. Transduced cells were selected with puromycin (Calbiochem; 1 to 2 µg/ml) or directly used in some superinfection experiments with pMRX-IP-GFP-LC3-RFP-LC3ΔG.

Flow cytometry analysis of autophagic flux: Cell transduced with MRX-IP-GFP-LC3-RFP-LC3ΔG vector were seeded at 4 x 10^5 cells per 6 cm diameter dish (day 0), treated at day 1 as indicated and dissociated and harvested in cold culture medium at day 2 by strong pipetting after Tryp-EDTA-Pyr treatment, pelleted by centrifugation, resuspended in 500 µL of cold PBS 1X and eventually fixed by adding 4.5 mL of 4 % paraformaldehyde in saline (sc-281692, Santa Cruz Biotechnology, France) and incubating at room temperature for 5 minutes. Then, cells were washed 2 times with PBS1X, suspended in 500 µL PBS 1X and kept at 4°C in dark until analysis. The GFP and RFP cell fluorescence was measured using a Fortessa Flow-cytometer (BD Biosciences) with excitation/emission at 488/515-545 and 561/600-620 nm respectively. For data analysis using FlowJo software (BD Biosciences), the RFP positive cell subpopulation was first selected to measure the GFP/RFP fluorescence ratio. The prior elimination of cell doublets did not have a significant impact the results.

mRNA isolation and RT-qPCR analysis: Cultured cells or spheroids were washed twice with cold PBS, and processed for total RNA isolation using the RNeasy Mini Kit (Qiagen, France) or Trizol reagent (Invitrogen, ThermoFisher Scientific, France). Tumor fragments were minced into fine pieces and lysed by vigorous shaking with steel balls in Trizol reagent. qRT-PCR experiments were performed as previously published [8, 10] using the LightCycler 480 SYBR Green I Master kit. *Hprt* was selected as the reference gene for normalization of data derived from independent cDNA synthesis reactions and normalization was further checked using others control gene such as *Sdha* or *Rplp0*. The expression level of each mRNA species was further normalized to that measured in the growing 2D-culture (KC-2D) set to 1. Oligonucleotide primers sequences along with a summary of data are shown in **S1 file**.

Western blot analysis: Cells were seeded at 4 x 10^5 cells per 6 cm diameter dish (day 0), treated at day 1 as indicated and lysed at day 2 or 3. For cell lysis, cells were washed two times with cold PBS1X and lysed in Laemli 2X lysis buffer supplemented with phosphatase inhibitors. About 50 µg protein lysate were subjected to SDS-PAGE and transferred to a polyvinylidene fluoride membrane (Hybond P; RPN303F from Amersham Pharmacia Biotech, England) that was blocked with 5% non-fat milk, in PBS1X containing 0.1% Tween-20 and probed with primary antibodies in the same buffer overnight at 4°C. Proteins were detected using horseradish peroxidase-conjugated secondary antibodies and detected using ECL (RPN2106) or ECL-select (RPN2235) reagents (Amersham, GE Healthcare, UK) and a cooled digital camera (LC33000, FujiFilm). Relative protein levels in each lane was measured using the Multi Gauge software (Fuji Microsoft, FujiFilm) associated to the digital camera device.

Animals models: The animal protocol used in this study was reviewed and approved by the local ethics committee (Comité d'Ethique en Expérimentation Animale of University of Paris; approved protocol CEEA 18-088 submitted by C. Nicco and T. Tchenio). Six-week-old female *NOD.CB-17-Prkdc scid/Rj* (NOD-SCID) or C57Bl/6 J mice weighing 16–20 g were purchased from Janvier Laboratory (Le Genest Saint Isle, France). All mice were housed in ventilated cages with sterile food and water *ad libitum* throughout the study. Animals received humane care in compliance with the guidelines implemented at our institution (INSERM and University Paris Descartes). The presence of subcutaneous tumors was carefully checked by palpation, light pinching and rolling of the skin between fingers to assess thickening of the skin and the presence of small hard lumps, which allowed to detect most of the tumors several days before they reach 1 mm^3. Tumor size was measured two times a week with Vernier calipers. Tumor volumes were calculated using the following formula: (L * W * W)/2, in which L represents the large diameter of the tumor, and W represents the small diameter.

Experimental procedures for NOD-SCID mice: KC-DT66066 cells in SSQ were generated in two steps. 4 x 10^5 cells were seeded in 6 cm diameter dish and treated the next day with Torin1 (200 nM) for 1 day. Cells were then subcultured at low cell density in growth medium with 1.9% FCS plus insulin 10 µg/mL (to enhance survival of cells in SSQ) for 3 days and then subjected to gemcitabine selection for 5 days in regular medium supplemented with gemcitabine at 30 ng/mL. Cells in SSQ were then harvested in DMEM with 10% fetal calf serum after 5 min treatment with Tryp-EDTA-Pyr solution warmed to 37°C, washed two times with cold DMEM without serum or antibiotics, resuspended in a small volume of DMEM and counted. Exponentially growing cells were harvested from 6 cm diameter dishes seeded with 4 x 10^5 cells two days before and harvested as cells in SSQ in DMEM. Harvested cells were injected subcutaneously in the backs of mice. The mouse treatments were gemcitabine 50

mg/kg injected intraperitoneally on day 4 and 11 for the Ssq/gem group, N-acetylcysteine 300 mg/kg injected intraperitoneally on days 4, 6, 8, 11, 13, 15 for the Ssq/NAC group, day 0 referring to the day of cell injection.

Experimental procedures for C57Bl/6 mice. Cells were seeded at 4 x 10^5 per 10 cm diameter plate and then cultured for 4 or 5 days with a growth medium change on the third day. Cells were harvested by a 3 min treatment with Tryp-EDTA-Pyr, washed twice with growth medium without serum or antibiotics, filtered through a 70 µm cell strainer and 200 µl of a cell suspension at 5 x 10^6 cells/mL subcutaneously injected (day 0) into the back of C57Bl/6 mice. Cyclosporin A (Sandoz, France) was administered orally at a dose of 80 mg/kg at days -2, 0, 4, 7 and 11.

Analysis of patients' records: The anonymized records from 144 patients with pancreatic adenocarcinoma (PAAD) included in the TGCA-PAAD project and with a follow up and a transcriptome profiling of their primary tumors by Illumina sequencing were downloaded from the Genomic Data Commons website as clinical files and FPKM transcriptome-sequencing files. For gene expression analysis, genes counts from the FPKM files were assembled into a count matrix K_{ij} (for gene i in tumor sample j) after filtering genes with zero geometric mean. Gene counts were normalized by calculating scaling factors analogous to those calculated in the DESeq package [50, 51]: $\lambda_j = \mathrm{MEDIAN}_{i=1 \text{ to } 17689}\{K_{ij}/\mathrm{GEOMETRIC_MEAN}_{k=1 \text{ to } 149}\{K_{ik}\}\}$. The normalized FPKM value K_{ij}/λ_j was used as a measure of the expression level of gene i in tumor j. In the case of 5 patients for whom there were 2 sequencing files, we took the geometric mean value of normalized gene counts. This normalization introduced in most cases only a small correction (the average value of λ_j was λ=1.01 ± 0.12, mean ± s.d.; n=149) and was validated *a posteriori* by the strong self-consistency of the results obtained. The cutoff value

θ used to categorize patients in cohorts with a low or high level of expression of a given gene in their tumor, was chosen to maximize the statistical significance of the difference in survival between the two cohorts of patients. For *BECN1* mRNA levels (8.56 ± 1.83 FPKM, mean ± s.d., range: 4.2-18.0, n=124), a cutoff value of 8.895 FPKM was used throughout this. For *CCNA2* mRNA levels (4.76 ± 2.86 FPKM, mean ± s.d., range: 1.12-16.44, n=124) a cutoff value of 5.66 FPKM was used throughout this study (see also **S2 file**).

The clinical data were verified by cross-referencing the various clinical files for the treatment status and for the duration of patient survival without local or distant tumor recurrence. Only the records of 124 of the 144 patients contained relevant indications on local recurrence and the status of distant metastasis. They include 109 patients with a pancreas adenocarcinoma of the ductal subtype, 6 with a Not Otherwise Stated subtype, 3 with a poorly differentiated and 1 with a well differentiated subtype, 3 with mixed phenotypes (ductal and micropapillary or neuroendocrine subtypes) and 2 with an invasive phenotype. The "Initial treatment" corresponded to removal of the primary tumor by partial or total pancreatectomy. Adjuvant chemotherapy was recorded for 78% of patients (the treatment status was not specified for the remaining patients) and this percentage increased to 89% for patients with distant metastasis-free survival >360 day. When a patient had a local recurrence or a new cancer type, he was censored at the time of that diagnostic in the Kaplan-Meier analysis for distant metastasis-free survival. Data were processed and analyzed using Excel (version 16; Microsoft, USA) upgraded with Real Statistics add-ins (Zaiontz, C., 2020, Real Statistics Using Excel.at www.real-statistics.com) and GraphPad Prism version 5.00 (San Diego, California, USA). Enrichment analysis was performed with Gene Set Enrichment Analysis software (GSEA v4.2.0 for Windows and Mac) with default settings and the msigdb.v7.4.symbols.gmt dataset available from the Broad Institute. Hierarchical gene clustering was performed using Morpheus software (https://software.broadinstitute.org/morpheus). The references of downloaded files and a

synthetic summary of clinical data are given in **S2 file**. Normalized sequencing data are provided in **S3 file**.

Statistics: In all graphs, each point corresponds to an independent measurement, the labels above the data points indicate the average values and error bars are standard deviation unless otherwise indicated. Significance was measured using a two-tailed Student's t-test unless otherwise specified. Log-ranked (Mantel-Cox) and Fisher's exact probability test were performed using GraphPad Prism version 5.00 (San Diego, California, USA). Correlations were calculated using Excel software (Microsoft Standard Office 2016) and their statistical significance calculated on the Vassar web site (http://vassarstats.net). Multivariate Cox regression analysis was performed using Excel (version 16; Microsoft, USA) upgraded with Real Statistics add-ins (Zaiontz, C., 2020, Real Statistics Using Excel.at www.real-statistics.com). The number of * indicates the statistical significance of the difference between the indicated mean values with * for $p<0.05$, ** for $p<10^{-2}$, *** for $p<10^{-3}$, **** for $p<10^{-4}$, ***** for $p<10^{-5}$ and ******* for $p<10^{-6}$ and the same for #.

Data Availability Statement: The authors declare that all data supporting the findings of this study are available within the article and its supplementary information, or available from the corresponding author upon reasonable request.

References

1. Luzzi KJ, MacDonald IC, Schmidt EE, Kerkvliet N, Morris VL, Chambers AF, et al. Multistep nature of metastatic inefficiency: dormancy of solitary cells after successful

extravasation and limited survival of early micrometastases. The American journal of pathology. 1998;153(3):865-73. PubMed PMID: 9736035.

2. Cameron MD, Schmidt EE, Kerkvliet N, Nadkarni KV, Morris VL, Groom AC, et al. Temporal progression of metastasis in lung: cell survival, dormancy, and location dependence of metastatic inefficiency. Cancer research. 2000;60(9):2541-6. PubMed PMID: 10811137.

3. Naumov GN, MacDonald IC, Weinmeister PM, Kerkvliet N, Nadkarni KV, Wilson SM, et al. Persistence of solitary mammary carcinoma cells in a secondary site: a possible contributor to dormancy. Cancer research. 2002;62(7):2162-8. PubMed PMID: 11929839.

4. McAllister SS, Gifford AM, Greiner AL, Kelleher SP, Saelzler MP, Ince TA, et al. Systemic endocrine instigation of indolent tumor growth requires osteopontin. Cell. 2008;133(6):994-1005. Epub 2008/06/17. doi: 10.1016/j.cell.2008.04.045. PubMed PMID: 18555776; PubMed Central PMCID: PMCPMC4121664.

5. Risson E, Nobre AR, Maguer-Satta V, Aguirre-Ghiso JA. The current paradigm and challenges ahead for the dormancy of disseminated tumor cells. Nat Cancer. 2020;1(7):672-80. Epub 2021/03/09. doi: 10.1038/s43018-020-0088-5. PubMed PMID: 33681821; PubMed Central PMCID: PMCPMC7929485.

6. Shen S, Vagner S, Robert C. Persistent Cancer Cells: The Deadly Survivors. Cell. 2020;183(4):860-74. Epub 2020/11/14. doi: 10.1016/j.cell.2020.10.027. PubMed PMID: 33186528.

7. Janni W, Rack B, Schindlbeck C, Strobl B, Rjosk D, Braun S, et al. The persistence of isolated tumor cells in bone marrow from patients with breast carcinoma predicts an increased risk for recurrence. Cancer. 2005;103(5):884-91. Epub 2005/01/25. doi: 10.1002/cncr.20834. PubMed PMID: 15666325.

8. Bui AT, Laurent F, Havard M, Dautry F, Tchenio T. SMAD signaling and redox imbalance cooperate to induce prostate cancer cell dormancy. Cell cycle. 2015;14(8):1218-31.

doi: 10.1080/15384101.2015.1014145. PubMed PMID: 25706341; PubMed Central PMCID: PMC4615032.

9. Havard M, Dautry F, Tchenio T. A dormant state modulated by osmotic pressure controls clonogenicity of prostate cancer cells. The Journal of biological chemistry. 2011;286(51):44177-86. doi: 10.1074/jbc.M111.262709. PubMed PMID: 22039055; PubMed Central PMCID: PMC3243505.

10. Bui AT, Huang ME, Havard M, Laurent-Tchenio F, Dautry F, Tchenio T. Transient exposure to androgens induces a remarkable self-sustained quiescent state in dispersed prostate cancer cells. Cell cycle. 2017;16(9):879-93. doi: 10.1080/15384101.2017.1310345. PubMed PMID: 28426320; PubMed Central PMCID: PMC5444360.

11. Baer R, Cintas C, Dufresne M, Cassant-Sourdy S, Schonhuber N, Planque L, et al. Pancreatic cell plasticity and cancer initiation induced by oncogenic Kras is completely dependent on wild-type PI 3-kinase p110alpha. Genes & development. 2014;28(23):2621-35. doi: 10.1101/gad.249409.114. PubMed PMID: 25452273; PubMed Central PMCID: PMC4248293.

12. Hingorani SR, Petricoin EF, Maitra A, Rajapakse V, King C, Jacobetz MA, et al. Preinvasive and invasive ductal pancreatic cancer and its early detection in the mouse. Cancer Cell. 2003;4(6):437-50. doi: 10.1016/s1535-6108(03)00309-x. PubMed PMID: 14706336.

13. Maciel-Baron LA, Morales-Rosales SL, Aquino-Cruz AA, Triana-Martinez F, Galvan-Arzate S, Luna-Lopez A, et al. Senescence associated secretory phenotype profile from primary lung mice fibroblasts depends on the senescence induction stimuli. Age (Dordrecht, Netherlands). 2016;38(1):26. Epub 20160211. doi: 10.1007/s11357-016-9886-1. PubMed PMID: 26867806; PubMed Central PMCID: PMCPMC5005892.

14. Fung C, Lock R, Gao S, Salas E, Debnath J. Induction of autophagy during extracellular matrix detachment promotes cell survival. Molecular biology of the cell. 2008;19(3):797-806.

doi: 10.1091/mbc.e07-10-1092. PubMed PMID: 18094039; PubMed Central PMCID: PMC2262959.

15. Kaizuka T, Morishita H, Hama Y, Tsukamoto S, Matsui T, Toyota Y, et al. An Autophagic Flux Probe that Releases an Internal Control. Molecular cell. 2016;64(4):835-49. doi: 10.1016/j.molcel.2016.09.037. PubMed PMID: 27818143.

16. Thoreen CC, Kang SA, Chang JW, Liu Q, Zhang J, Gao Y, et al. An ATP-competitive mammalian target of rapamycin inhibitor reveals rapamycin-resistant functions of mTORC1. The Journal of biological chemistry. 2009;284(12):8023-32. Epub 20090115. doi: 10.1074/jbc.M900301200. PubMed PMID: 19150980; PubMed Central PMCID: PMCPMC2658096.

17. Wirawan E, Lippens S, Vanden Berghe T, Romagnoli A, Fimia GM, Piacentini M, et al. Beclin1: a role in membrane dynamics and beyond. Autophagy. 2012;8(1):6-17. Epub 2011/12/16. doi: 10.4161/auto.8.1.16645. PubMed PMID: 22170155.

18. Hosokawa N, Hara T, Kaizuka T, Kishi C, Takamura A, Miura Y, et al. Nutrient-dependent mTORC1 association with the ULK1-Atg13-FIP200 complex required for autophagy. Molecular biology of the cell. 2009;20(7):1981-91. Epub 20090211. doi: 10.1091/mbc.E08-12-1248. PubMed PMID: 19211835; PubMed Central PMCID: PMCPMC2663915.

19. Di Bartolomeo S, Corazzari M, Nazio F, Oliverio S, Lisi G, Antonioli M, et al. The dynamic interaction of AMBRA1 with the dynein motor complex regulates mammalian autophagy. The Journal of cell biology. 2010;191(1):155-68. Epub 2010/10/06. doi: 10.1083/jcb.201002100. PubMed PMID: 20921139; PubMed Central PMCID: PMCPMC2953445.

20. Vadlakonda L, Dash A, Pasupuleti M, Anil Kumar K, Reddanna P. The Paradox of Akt-mTOR Interactions. Frontiers in oncology. 2013;3:165. Epub 20130620. doi:

10.3389/fonc.2013.00165. PubMed PMID: 23802099; PubMed Central PMCID: PMCPMC3687210.

21. Mauvezin C, Neufeld TP. Bafilomycin A1 disrupts autophagic flux by inhibiting both V-ATPase-dependent acidification and Ca-P60A/SERCA-dependent autophagosome-lysosome fusion. Autophagy. 2015;11(8):1437-8. doi: 10.1080/15548627.2015.1066957. PubMed PMID: 26156798; PubMed Central PMCID: PMCPMC4590655.

22. Deshmukh SK, Tyagi N, Khan MA, Srivastava SK, Al-Ghadhban A, Dugger K, et al. Gemcitabine treatment promotes immunosuppressive microenvironment in pancreatic tumors by supporting the infiltration, growth, and polarization of macrophages. Sci Rep. 2018;8(1):12000. Epub 20180810. doi: 10.1038/s41598-018-30437-2. PubMed PMID: 30097594; PubMed Central PMCID: PMCPMC6086900.

23. Liberzon A, Birger C, Thorvaldsdottir H, Ghandi M, Mesirov JP, Tamayo P. The Molecular Signatures Database (MSigDB) hallmark gene set collection. Cell Syst. 2015;1(6):417-25. doi: 10.1016/j.cels.2015.12.004. PubMed PMID: 26771021; PubMed Central PMCID: PMCPMC4707969.

24. Cianfanelli V, Fuoco C, Lorente M, Salazar M, Quondamatteo F, Gherardini PF, et al. AMBRA1 links autophagy to cell proliferation and tumorigenesis by promoting c-Myc dephosphorylation and degradation. Nature cell biology. 2015;17(1):20-30. Epub 20141201. doi: 10.1038/ncb3072. PubMed PMID: 25438055; PubMed Central PMCID: PMCPMC4976803.

25. Maiani E, Milletti G, Nazio F, Holdgaard SG, Bartkova J, Rizza S, et al. AMBRA1 regulates cyclin D to guard S-phase entry and genomic integrity. Nature. 2021;592(7856):799-803. Epub 20210414. doi: 10.1038/s41586-021-03422-5. PubMed PMID: 33854232; PubMed Central PMCID: PMCPMC8864551.

26. Simoneschi D, Rona G, Zhou N, Jeong YT, Jiang S, Milletti G, et al. CRL4(AMBRA1) is a master regulator of D-type cyclins. Nature. 2021;592(7856):789-93. Epub 20210414. doi: 10.1038/s41586-021-03445-y. PubMed PMID: 33854235; PubMed Central PMCID: PMCPMC8875297.

27. Thoresen SB, Pedersen NM, Liestol K, Stenmark H. A phosphatidylinositol 3-kinase class III sub-complex containing VPS15, VPS34, Beclin 1, UVRAG and BIF-1 regulates cytokinesis and degradative endocytic traffic. Experimental cell research. 2010;316(20):3368-78. Epub 20100717. doi: 10.1016/j.yexcr.2010.07.008. PubMed PMID: 20643123.

28. Rohatgi RA, Janusis J, Leonard D, Bellve KD, Fogarty KE, Baehrecke EH, et al. Beclin 1 regulates growth factor receptor signaling in breast cancer. Oncogene. 2015;34(42):5352-62. Epub 2015/02/03. doi: 10.1038/onc.2014.454. PubMed PMID: 25639875; PubMed Central PMCID: PMCPMC4522409.

29. Matthew-Onabanjo AN, Janusis J, Mercado-Matos J, Carlisle AE, Kim D, Levine F, et al. Beclin 1 Promotes Endosome Recruitment of Hepatocyte Growth Factor Tyrosine Kinase Substrate to Suppress Tumor Proliferation. Cancer research. 2020;80(2):249-62. Epub 2019/11/21. doi: 10.1158/0008-5472.CAN-19-1555. PubMed PMID: 31744816; PubMed Central PMCID: PMCPMC6980665.

30. Song X, Zhu S, Chen P, Hou W, Wen Q, Liu J, et al. AMPK-Mediated BECN1 Phosphorylation Promotes Ferroptosis by Directly Blocking System Xc(-) Activity. Current biology : CB. 2018;28(15):2388-99 e5. Epub 20180726. doi: 10.1016/j.cub.2018.05.094. PubMed PMID: 30057310; PubMed Central PMCID: PMCPMC6081251.

31. Hu F, Li G, Huang C, Hou Z, Yang X, Luo X, et al. The autophagy-independent role of BECN1 in colorectal cancer metastasis through regulating STAT3 signaling pathway activation. Cell death & disease. 2020;11(5):304. Epub 2020/05/03. doi: 10.1038/s41419-020-2467-3. PubMed PMID: 32358527; PubMed Central PMCID: PMCPMC7195408.

32. Reiling JH, Sabatini DM. Stress and mTORture signaling. Oncogene. 2006;25(48):6373-83. doi: 10.1038/sj.onc.1209889. PubMed PMID: 17041623.

33. Alexander A, Cai SL, Kim J, Nanez A, Sahin M, MacLean KH, et al. ATM signals to TSC2 in the cytoplasm to regulate mTORC1 in response to ROS. Proceedings of the National Academy of Sciences of the United States of America. 2010;107(9):4153-8. doi: 10.1073/pnas.0913860107. PubMed PMID: 20160076; PubMed Central PMCID: PMC2840158.

34. Watson A, Lipina C, McArdle HJ, Taylor PM, Hundal HS. Iron depletion suppresses mTORC1-directed signalling in intestinal Caco-2 cells via induction of REDD1. Cellular signalling. 2016;28(5):412-24. Epub 20160129. doi: 10.1016/j.cellsig.2016.01.014. PubMed PMID: 26827808; PubMed Central PMCID: PMCPMC4804389.

35. Pant K, Saraya A, Venugopal SK. Oxidative stress plays a key role in butyrate-mediated autophagy via Akt/mTOR pathway in hepatoma cells. Chemico-biological interactions. 2017;273:99-106. Epub 20170612. doi: 10.1016/j.cbi.2017.06.001. PubMed PMID: 28600122.

36. Oka SI, Hirata T, Suzuki W, Naito D, Chen Y, Chin A, et al. Thioredoxin-1 maintains mechanistic target of rapamycin (mTOR) function during oxidative stress in cardiomyocytes. The Journal of biological chemistry. 2017;292(46):18988-9000. Epub 20170922. doi: 10.1074/jbc.M117.807735. PubMed PMID: 28939765; PubMed Central PMCID: PMCPMC5704480.

37. Romero AM, Ramos-Alonso L, Montella-Manuel S, Garcia-Martinez J, de la Torre-Ruiz MA, Perez-Ortin JE, et al. A genome-wide transcriptional study reveals that iron deficiency inhibits the yeast TORC1 pathway. Biochim Biophys Acta Gene Regul Mech. 2019;1862(9):194414. Epub 20190805. doi: 10.1016/j.bbagrm.2019.194414. PubMed PMID: 31394264.

38. Daher B, Parks SK, Durivault J, Cormerais Y, Baidarjad H, Tambutte E, et al. Genetic Ablation of the Cystine Transporter xCT in PDAC Cells Inhibits mTORC1, Growth, Survival, and Tumor Formation via Nutrient and Oxidative Stresses. Cancer research. 2019;79(15):3877-90. Epub 20190607. doi: 10.1158/0008-5472.CAN-18-3855. PubMed PMID: 31175120.

39. Zhou J, Li XY, Liu YJ, Feng J, Wu Y, Shen HM, et al. Full-coverage regulations of autophagy by ROS: from induction to maturation. Autophagy. 2021:1-16. Epub 20211018. doi: 10.1080/15548627.2021.1984656. PubMed PMID: 34662529.

40. Brielmeier M, Bechet JM, Falk MH, Pawlita M, Polack A, Bornkamm GW. Improving stable transfection efficiency: antioxidants dramatically improve the outgrowth of clones under dominant marker selection. Nucleic Acids Res. 1998;26(9):2082-5. Epub 1998/06/20. PubMed PMID: 9547263; PubMed Central PMCID: PMC147536.

41. Almog N. Molecular mechanisms underlying tumor dormancy. Cancer Lett. 2010;294(2):139-46. Epub 20100402. doi: 10.1016/j.canlet.2010.03.004. PubMed PMID: 20363069.

42. Cianfanelli V, D'Orazio M, Cecconi F. AMBRA1 and BECLIN 1 interplay in the crosstalk between autophagy and cell proliferation. Cell cycle. 2015;14(7):959-63. Epub 2015/03/25. doi: 10.1080/15384101.2015.1021526. PubMed PMID: 25803737; PubMed Central PMCID: PMCPMC4615147.

43. Liang XH, Jackson S, Seaman M, Brown K, Kempkes B, Hibshoosh H, et al. Induction of autophagy and inhibition of tumorigenesis by beclin 1. Nature. 1999;402(6762):672-6. doi: 10.1038/45257. PubMed PMID: 10604474.

44. Wechman SL, Pradhan AK, DeSalle R, Das SK, Emdad L, Sarkar D, et al. New Insights Into Beclin-1: Evolution and Pan-Malignancy Inhibitor Activity. Advances in cancer research. 2018;137:77-114. Epub 20171227. doi: 10.1016/bs.acr.2017.11.002. PubMed PMID: 29405978; PubMed Central PMCID: PMCPMC7645729.

45. Kim HS, Lee SH, Do SI, Lim SJ, Park YK, Kim YW. Clinicopathologic correlation of beclin-1 expression in pancreatic ductal adenocarcinoma. Pathol Res Pract. 2011;207(4):247-52. Epub 2011/03/23. doi: 10.1016/j.prp.2011.02.007. PubMed PMID: 21420796.

46. Song S, Wang B, Gu S, Li X, Sun S. Expression of Beclin 1 and Bcl-2 in pancreatic neoplasms and its effect on pancreatic ductal adenocarcinoma prognosis. Oncology letters. 2017;14(6):7849-61. Epub 2018/01/19. doi: 10.3892/ol.2017.7218. PubMed PMID: 29344231; PubMed Central PMCID: PMCPMC5755265.

47. Takahashi Y, Coppola D, Matsushita N, Cualing HD, Sun M, Sato Y, et al. Bif-1 interacts with Beclin 1 through UVRAG and regulates autophagy and tumorigenesis. Nature cell biology. 2007;9(10):1142-51. Epub 2007/09/25. doi: 10.1038/ncb1634. PubMed PMID: 17891140; PubMed Central PMCID: PMCPMC2254521.

48. Vera-Ramirez L, Vodnala SK, Nini R, Hunter KW, Green JE. Autophagy promotes the survival of dormant breast cancer cells and metastatic tumour recurrence. Nature communications. 2018;9(1):1944. Epub 2018/05/24. doi: 10.1038/s41467-018-04070-6. PubMed PMID: 29789598; PubMed Central PMCID: PMCPMC5964069.

49. Sancak Y, Peterson TR, Shaul YD, Lindquist RA, Thoreen CC, Bar-Peled L, et al. The Rag GTPases bind raptor and mediate amino acid signaling to mTORC1. Science (New York, NY). 2008;320(5882):1496-501. Epub 2008/05/24. doi: 10.1126/science.1157535. PubMed PMID: 18497260; PubMed Central PMCID: PMCPMC2475333.

50. Anders S, Huber W. Differential expression analysis for sequence count data. Nature Precedings. 2010. doi: 10.1038/npre.2010.4282.1.

51. Dillies MA, Rau A, Aubert J, Hennequet-Antier C, Jeanmougin M, Servant N, et al. A comprehensive evaluation of normalization methods for Illumina high-throughput RNA sequencing data analysis. Brief Bioinform. 2013;14(6):671-83. Epub 20120917. doi: 10.1093/bib/bbs046. PubMed PMID: 22988256.

Supplemental material

S1 Fig. Selection of cancer cells in SSQ with anticancer agents in pancreas and prostate cancer cell lines cultured at clonogenic cell density.

S2 Fig. SSQ induction is regulated by mTOR and Beclin-1 but not autophagy.

S3 Fig. Tumorigenicity of KC cells injected subcutaneously in mice.

S4 Fig. Beclin-1 and Cyclin A2 transcript levels in the primary tumor of PAAD patients are predictive of early and late metastasis.

S1 file: Sequences of primers used for RT-qPCR analysis and summary of RT-qPCR expression data.

S2 file: Synthetic summary of clinical and sequencing data including references of clinical and sequencing files retrieved from the Genomic Data Commons website.

S3 file: Genes count matrix derived from the 149 FPKM sequencing files (retrieved from the Genomic Data Commons website) and normalized by scaling factors λ_{ij}. See the Methods section for explanations.

Author contributions

Conceptualization: TT. Supervision: CN, FB, TT. Methodology: TT. Investigation: JG provided murine pancreas cancer cell lines derived from corresponding transgenic mice; MH carried out counting of colonies from clonogenic assays and plasmids constructions in studies with prostate cancer cells. TT performed cell culture, flow cytometry qPCR, Western Blot experiments and analysis of patients' records; CN and MT carried out animal experiments. Formal analysis: T.T; Analysis and Visualization of Data: FB, CN, TT. Writing original draft: TT. Review and Editing: CN, FB, FD, FLT, JG, LD and TT. No grant funded this study.

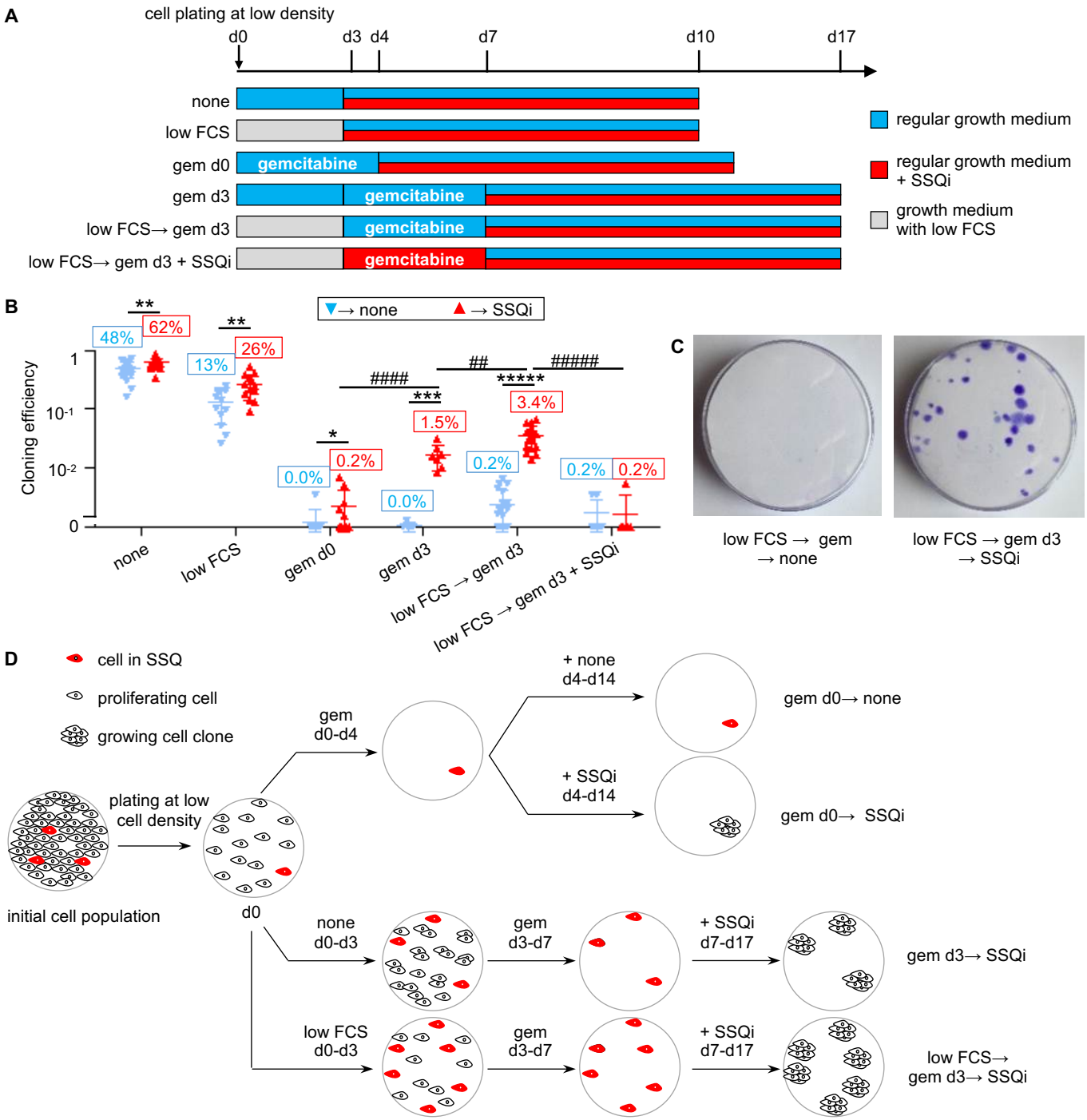

Fig 1: **Selection of pancreas cancer KC-DT66066 cells in SSQ at low cell density with anticancer agents. A)** Outlines of cloning efficiency (CE) assays to assess the kinetics of SSQ formation. Cells were plated at low cell density on day 0 (d0) and cultured as indicated. The labels on the left are those used in histograms. SSQi is a mixture of pharmacological agents that reverts SSQ (see Methods). **B)** Kinetics of the generation of gemcitabine-resistant cells. Histograms of CE measured with the indicated assays. Labels above bars indicate the percentage of seeded cells having formed a cell clone. * indicates the statistical significance of the change in CE induced by SSQi supplementation and # the statistical significance of the difference in CE between the indicated clonogenic assays with SSQi supplementation. **C)** Representative pictures of fixed and stained cell culture dishes after culturing the cells as indicated. **D)** Rationale for determining the relative frequency at which cancer cells in a cell population are in SSQ or are induced to enter SSQ by low cell density and low FCS. The gem d0 clonogenic assay selects cells that were already in SSQ in the initial cell population. SSQ cells switch to a proliferating state and formed cell clones after the addition of SSQi (gem d0→ SSQi clonogenic assay). Growing cell clones obtained in clonogenic assays with delayed gemcitabine selection and SSQi supplementation (gem d3→ SSQi and low FCS→ gem d3→ SSQi) originated from cells already in SSQ in the initial population or that entered SSQ after cell subculturing at low cell density or at low cell density and in low serum.

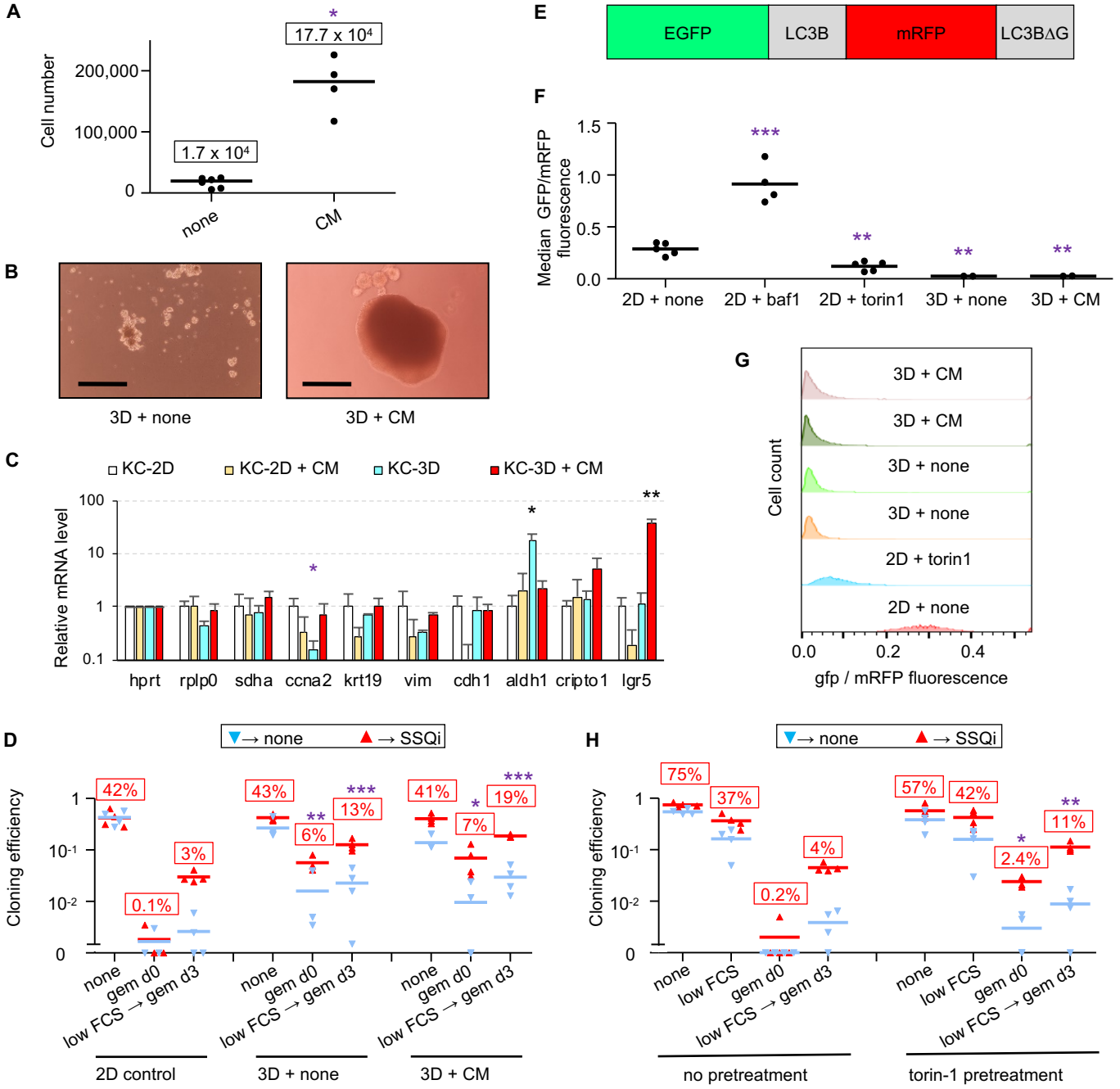

Fig 2: KC-DT66066 cell competence for entering SSQ is enhanced by 3D cell culture or treatment with pharmacological inhibitors of mTOR in 2D cell cultures. **A)** Growth of cells seeded at 10^4 cells per well in cell-repellent surface 12-well plate and cultured for 10 days in regular growth medium supplemented with none (none) and 50% conditioned medium (CM) from senescent mouse embryo fibroblasts cultures. The stars indicate the statistical significance of the differences with cells grown in regular growth medium. Labels indicate mean cell number. **B)** Representative pictures of cells grown for 7 days in cell-repellent surface plates in regular growth medium supplemented with none (3D + none) or Conditioned Medium (3D + CM). The scale bar indicates 0.25 mm. **C)** RT-qPCR analysis of mRNA species levels according to the indicated cell-culture conditions. Stars indicate statistical significance of differences with the KC-2D condition (n=4 independent experiments). **D)** CE of cells harvested from 3D or 2D cultures that were dissociated by the same method. The relatively high frequency of cell clones in the clonogenic assays gem d0→ none and low FCS→ gem d3→ none resulted from the spontaneous reversion of cells in SSQ after gemcitabine selection when their density exceeded 10% of the seeded cells. **E)** Schematic representation of the fusion protein encoded by the reporter gene EGFP-LC3B-mRFP-LC3BΔG encoding the autophagy sensitive EGFP-LC3B and the autophagy resistant mRFP-LC3ΔG fluorescent proteins.

Fig 2 continued: F) GFP to mRFP fluorescence ratio in EGFP-LC3B-mRFP-LC3BDG transduced cells cultured in 2D with none, bafilomycin A1 (baf1) or Torin1 for 1 day or cultured in 3D with none (3D+none) or CM (3D+CM) for 7 days. Stars indicate the significance of the difference with untreated 2D-cultured (control) cells. **G**) Data from a representative flow cytometry experiment showing the distribution of the ratio of GFP to mRFP fluorescence in transduced cells cultured as indicated. **H)** CE of cells pretreated at medium cell density in 2D-cultures with none or Torin1 for 1 day (pretreatment) before cell harvesting for CE assay. Labels above bars indicate the percentage of seeded cells having formed a cell clone after SSQi supplementation. Stars indicate statistical significance of CE differences with 2D control in panel **D** and with non-pretreated cells in panel **H** in clonogenic assays with SSQi supplementation.

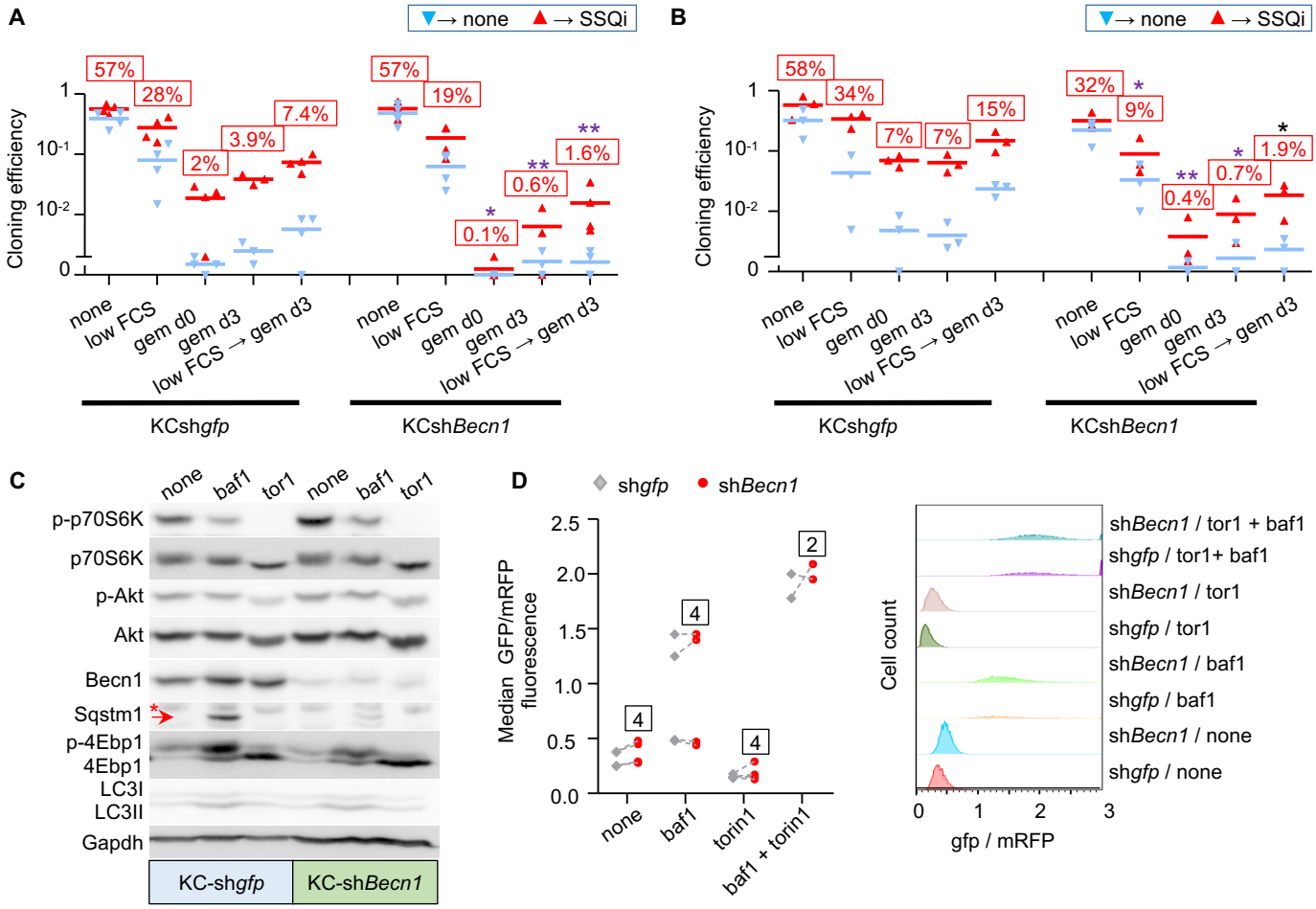

Fig 3: Beclin-1 downregulation inhibits SSQ but not autophagy. A) and **B)** CE of KC-DT66066 cell populations transduced with shRNA targeting GFP (KCsh*gfp*) or Beclin-1 (KCsh*becn1*) and pretreated with none **(A)** or Torin1 (**B**) as depicted in Fig 2H. Labels above bars indicate the percentage of seeded cells having formed a cell clone after SSQi supplementation. * indicate statistical significance (p) of CE differences after SSQi supplementation between KCsh*gfp* and KCsh*becn1* cells. **C**) Western Blot analysis of KCsh*gfp* and KCsh*Becn1* cell populations seeded at medium cell density at d0 and treated from d1 to d2 as indicated (baf1 and tor1 were for bafilomycin A1 and Torin1 respectively). This is one representative western blot of 3 analyzed. The star indicates a non-specific band and the arrow the SQSTM1 band. **D**) *left*: GFP/mRFP fluorescence ratio showing no difference in autophagic flux in KC*shgfp* and KC*shbecn1* cell populations transduced with the EGFP-LC3B-mRFP-LC3BΔG reporter gene. Cells were passaged at medium cell density at d0, treated from d1 to d2 with the indicated drugs (none, bafilomycin A1 (baf1), and/or Torin1) and analyzed as in Fig 2F-G. Dotted lines connect data points derived from a same experiment. Labels indicate the number of independent reporter gene transduction experiments. *Right*: A representative flow cytometry experiment shown.

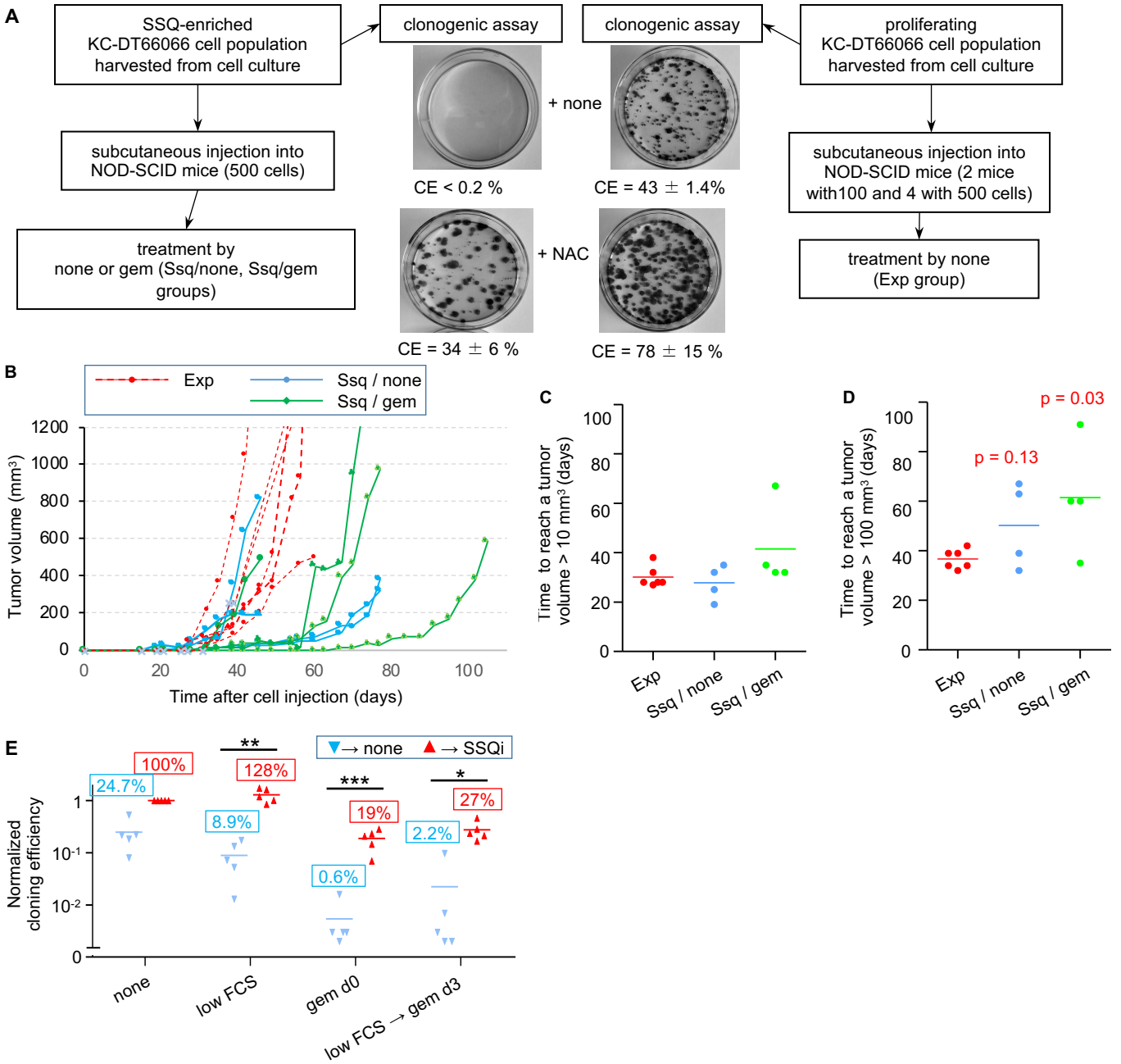

Fig 4: SSQ regulates tumor development. A) Outlines of the experiment performed to compare tumorigenicity of KC-DT66066 cells in a proliferating state or enriched for SSQ. **B)** Tumor growth curves in individual NOD-SCID mice subcutaneously injected with proliferating KC-DT66066 cells (Exp group, n=6) or with cells in SSQ and treated with none (Ssq / none group, n=4) or gemcitabine (Ssq / gem group; n=4). **C**) and **D**) Scatter plots showing the time taken for tumors to reach a volume of 10 mm^3 (**C**) or 100 mm^3 (**D**). p indicates the statistical significance of the difference in the proportion of mice with a slow tumor growth rate as calculated with a Fisher's exact probability test. Note that a third tumor in the Ssq/none group showed a slow tumor growth rate but only after having reached 200 mm^3 (see Fig 4B and main text). **E**) Growing tumors contain a significant percentage of cancer cells in SSQ or prone to enter SSQ. Clonogenic assays using cells dissociated from growing tumor resected from mice in the Exp (n=1), Ssq/none (n=2) and Ssq/gem (n=2) groups and directly tested for SSQ as described in Fig 1A. Data were normalized to 100% of cloning efficiency in the none → SSQi clonogenic assay. * indicates the statistical significance of the change in CE induced by SSQi supplementation. Note that spontaneous reversion of SSQ (that could be observed with the clonogenic assay low FCS → gem→ none) strongly increased in some dishes containing a high absolute number of cells in SSQ as observed in Fig 2D.

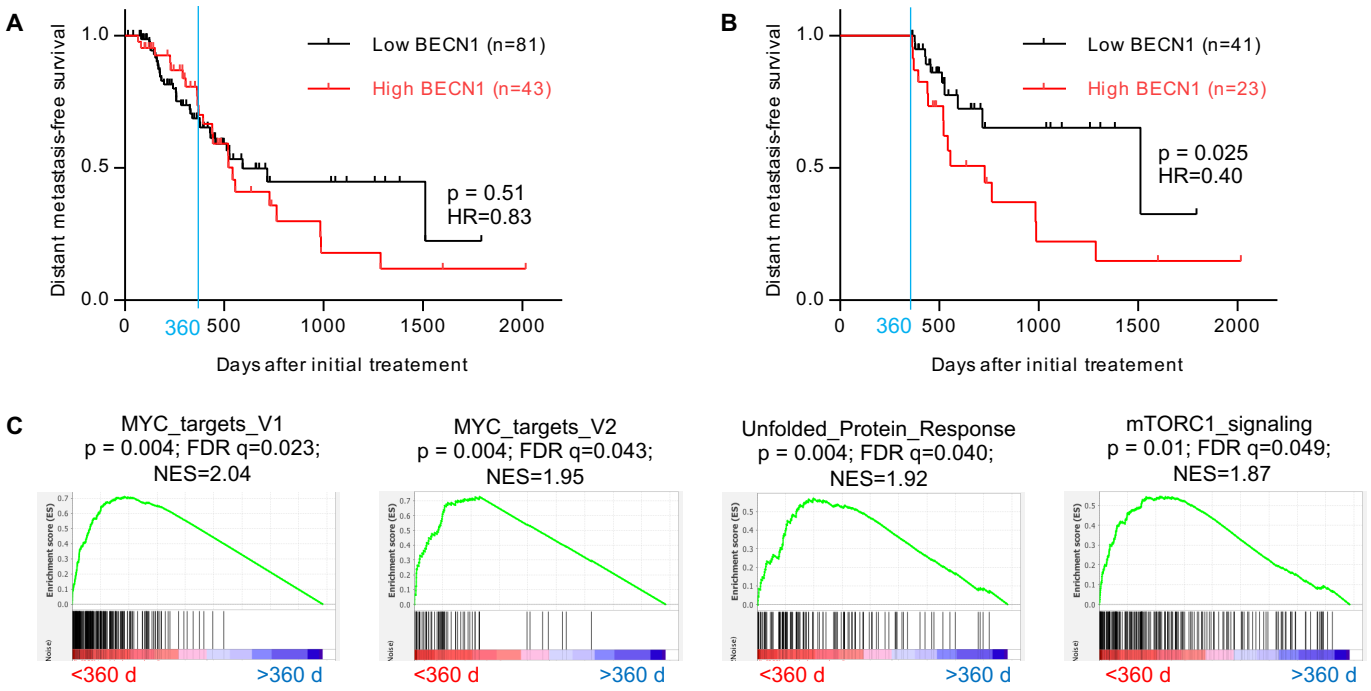

Fig 5: Elevated Beclin-1 expression in the primary tumor of PAAD patients is associated with an increased rate of metastasis in the patient cohort with a metastasis-free survival greater than 360 days. A) Kaplan-Meier curves for distant metastasis-free survival in PAAD patients according to the level of Beclin-1 transcripts in their primary tumor. **B)** Same as **(A)** but restricted to patients with survival time greater than 360 days. Initial treatment was partial or total pancreatectomy to remove the tumor and at least 78% of patients received adjuvant pharmaceutical treatments (see **S2 file**). Significance (p) of the difference in survival and hazard ratio (HR) were calculated with a Mantel-Cox Log-ranked test. **C)** Gene set enrichment analysis showing significant enrichment for hallmarks of MYC, mTORC1 and unfolded protein response signaling activity [23] in primary tumors of PAAD patients with a distant-metastasis-free survival time less than 360 days after initial treatment (n=60) *versus* greater than 360 days (n=64). Normalized enrichment score (NES), its statistical significance (p) and its false discovery rate (FDR) are indicated.

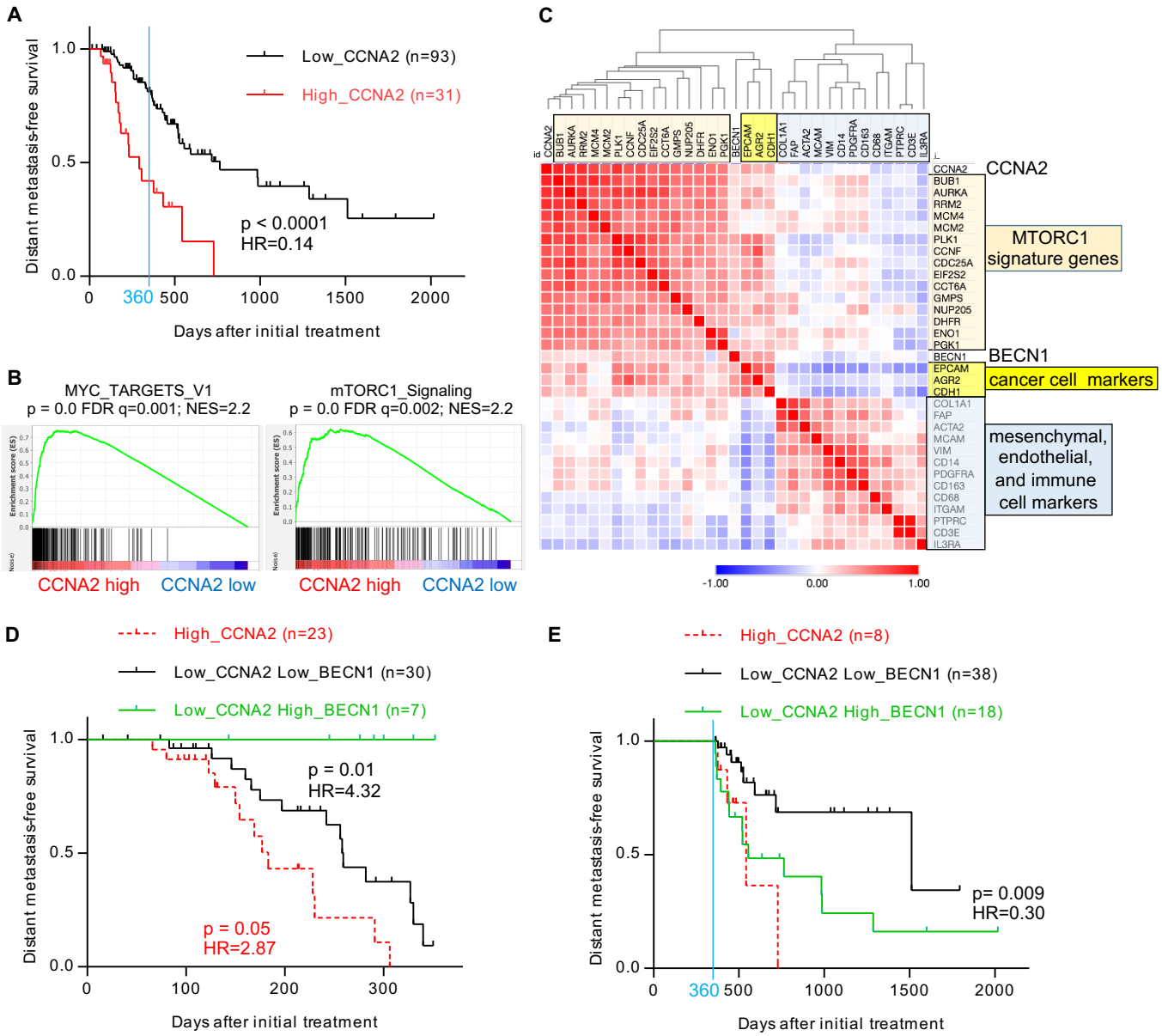

Fig 6: Cyclin A2 marks tumors with elevated mTORC1 activity and combines with Beclin-1 to predict kinetics of metastases development. A) Kaplan-Meier curves for distant metastasis-free survival in PAAD patients with high or low level of Cyclin A2 (*CCNA2*) transcripts in their primary tumor. **B)** GSEA demonstrates significant enrichment for hallmarks of cell proliferation and mTORC1 signaling [23] in the primary tumors of PAAD patients with high level (n=31) versus low level (n=93) of *CCNA2* transcripts. Normalized enrichment score (NES), its statistical significance (p) and its false discovery rate (FDR) are indicated. **C)** Hierarchical clustering of genes according to the Pearson correlation of their transcription levels in the primary tumors of PAAD patients (n=124). The colors indicate the value of the Pearson correlation coefficient for a given gene pair, ranging from -1 (blue) to +1 (red). The mTORC1 genes markers correspond to the first 15 highest ranked genes composing the mTORC1 signaling signature derived by GSEA analysis of PAAD tumors in Fig 5C (gene set M5924; [23]). **D)** Kaplan-Meier curves for distant metastasis-free survival in PAAD patients with survival time less than 360 days according to the transcript levels of cyclin A2 (CCNA2) and Beclin 1 (BCEN1) in their primary tumor. **E)** Same as panel D), but limited to patients with a survival time greater than 360 days. Log-ranked (Mantel-Cox) test was used to calculate the statistical significance (p) of the differences in distant metastasis-free survival between adjacent survival curves and hazard ratios (HR).

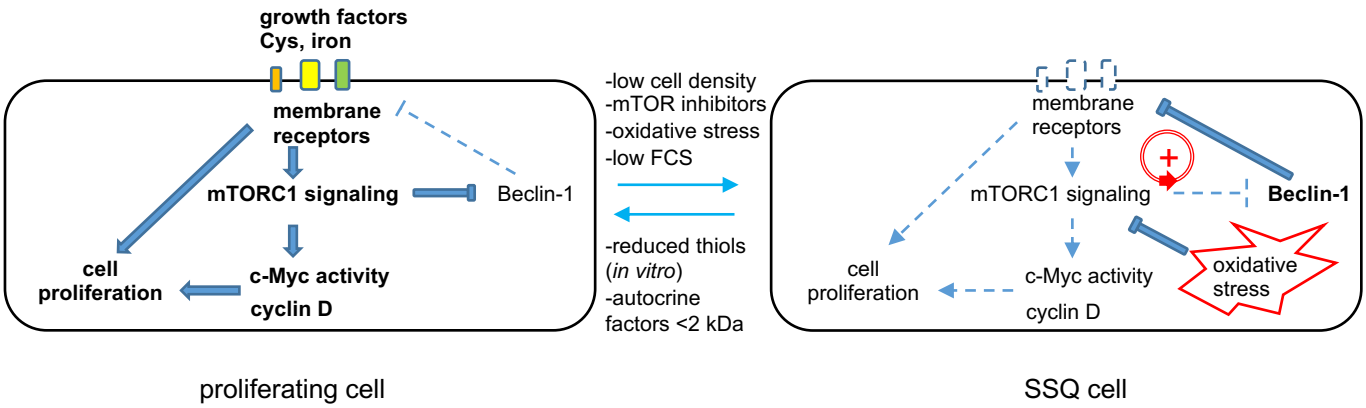

Fig 7: A molecular model of self-sustained quiescence. mTORC1 is a central node in the regulatory network controlling cell proliferation, for instance by regulating c-Myc activity, cyclin D accumulation and protein synthesis. Activation of Beclin-1 by downregulation of mTORC1 activity leads to activation of a regulatory loop (red circle in right panel) maintaining low mTORC1 activity. Indeed, Beclin-1 induced the degradation of cell surface receptor for growth factors and iron (transferrin receptor), and directly inhibits the Xc- cystine/glutamate antiporter [17, 27-30], which inhibits mTOR activity via nutrient depletion, oxidative stress and suppression of growth factors signaling pathways [32-39]. This model account for SSQ induction by low cell density that promotes oxidative stress [10, 40] and dilution of autocrine growth factors, mTOR inhibitors via Beclin-1-dependent but autophagy-independent pathways, low serum, for unresponsiveness of cancer cells in SSQ to growth factors and for the in vitro reversion of SSQ induced by reduced thiols. Note that BMP signaling stabilized SSQ in prostate cancer cells [8, 10] but appears to play a minor role in PAAD cells (see Methods for details and data not shown). The bold corresponds to activated signaling pathways while the dotted line corresponds to repressed pathways.